ADDIS ABABA UNIVERSITY

SCHOOL OF GRADUATE STUDIES

ADDIS ABABA INSTITUTE OF TECHNOLOGY

SCHOOL OF ELECTRICAL AND COMPUTER ENGINEERING

Performance Evaluation of Pilot-based Channel Estimation Techniques at Higher Modulation Order for LTE MIMO Downlink System

By: Daniel Berhan

Advisor: Dr. –Ing. Dereje Hailemariam

A thesis submitted to the school of Graduate studies of Addis Ababa University in partial fulfillment of the requirements for the degree of

Masters of Science

in

Communication Engineering

February, 2016

ADDIS ABABA UNIVERSITY

SCHOOL OF GRADUATE STUDIES

ADDIS ABABA INSTITUTE OF TECHNOLOGY

SCHOOL OF ELECTRICAL AND COMPUTER ENGINEERING

Performance Evaluation of Pilot-based Channel Estimation Techniques at Higher Modulation Order for LTE MIMO Downlink System

By: Daniel Berhan

APPROVAL BY BOARD OF EXAMINERS

Chairman School Graduate Committee	Signature
Advisor	Signature
Examiner	Signature
Examiner	Signature

I, the undersigned, declare that this thesis is my original work, has not been presented for a degree in this or any other university, and all sources of materials used for the thesis have been fully acknowledged.

Name: Daniel Berhan

Signature:_____

Place: Addis Ababa

Date of Submission: _____

This thesis has been submitted for examination with my approval as a university advisor.

Dr. –Ing. Dereje Hailemariam _____

Advisor Name Signature

Abstract

The number of smartphone users is increasing with increase in demand for high data rate. To fulfill this growing data rate demand, Long Term Evolution (LTE) is one technology option that is being widely deployed nowadays. LTE uses Orthogonal Frequency Division Multiplexing (OFDM) in the downlink system as its modulation scheme and multiple-input multiple-output (MIMO) antenna to achieve the high data rate. OFDM has the advantage over the conventional single-carrier modulation schemes when the channel is *frequency-selective fading* and is widely used in current wireless networks.

There are different types of data detection methods used in the current wireless technology. However, detection without the knowledge of the channel state information (CSI) is challenging and if not impossible. This is because of the fact that the transmission channel between a transmitter and a receiver can vary be from a simple line-of-sight to a severely faded one by multipath fading; moreover, the channel is random and time varying in nature. Hence, channel estimation methods are required to acquire the CSI. LTE uses cell-specific reference signals (CRS) or known pilots to estimate the channel properties.

Different pilot-based channel estimation techniques are developed over the last few decades. These include Least Square (LS) and Linear Minimum Mean Square Error (LMMSE) algorithms. Previous work on channel estimation is limited to single-input single-output (SISO)-OFDM and MIMO-OFDM systems in combination with lower modulation schemes like binary phase shift keying (BPSK) and quadrature phase shift keying (QPSK). Further study is required to understand the performance of MIMO-OFDM technology in LTE and at higher order modulation schemes that include 16 quadrature amplitude modulation (QAM) and 64 QAM.

This thesis investigates the performance of higher-order modulation schemes for the downlink of LTE based on MIMO-OFDM. LS and LMMSE channel estimation algorithms are considered at the receiver. Moreover, international telecommunication union (ITU) channel models such as extended pedestrian A model (EPA), extended vehicular A model (EVA) and extended typical urban (ETU) are used to characterize the propagation environment. Simulation results show that,

LMMSE has a higher gain than LS; however, the relative gain diminishes at higher SNR regions, specifically for SNR >30 dB. Similar results were reported in previous researches for the same system and channel model types but for lower order modulations.

Key words: - *LTE, pilot-based channel estimation, MIMO, EPA, EVA, ETU*

Acknowledgment

Firstly, I would like to thank God for giving me the knowledge and strength to finalize this thesis study.

I would like to express my sincere gratitude to my advisor Dr. –Ing. Dereje Hailemariam for his continuous support, patience, motivation and immense knowledge. His guidance helped me in all the time of research and writing of this thesis. I could not have imagined having a better advisor for this thesis study.

I would like to thank my wife Tayech Gashaw and my family for supporting and carrying me through their prayer throughout this thesis study. Last but not least, I thank my friends Daniel Retta and Beneyam Hailegnaw for their encouragement and support in providing me the necessary related documents.

Contents

List of Figures

List of Tables

List of Abbreviations

3GPP	3rd Generation Partnership Project
AWGN	Additive White Gaussian Noise
BER	Bit Error Rate
BPSK	Binary Phase Shift Keying
CDD	Cyclic Delay Diversity
CP	Cyclic Prefix
CRS	Cell-specific reference signals
CSI	Channel state information
DFT	Discrete Fourier Transform
DQPSK	Differential Quadrature Phase Shift Keying
DwPTS	Downlink Pilot Time Slot
EGC	Equal gain combining
eNodeB	Evolved Node B
EPA	Extended Pedestrian A Model
EPS	Evolved Packet System
ETU	Extended Typical urban Model
EVA	Extended Vehicular A Model
FDD	Frequency Division Duplex
FFT	Fast Fourier Transform
FSTD	Frequency Switched Transmit Diversity
GI	Guard Interval
GP	Guard Period
ICI	Inter Carrier Interference
IDFT	Inverse Discrete Fourier Transform
IFFT	Inverse Fast Fourier Transform
ISI	Inter Symbol Interference
ITU	International Telecommunication Union
LMMSE	Linear Minimum Mean Square Error
LS	Least Square

LTE	Long Term Evolution
MIMO	Multiple Input Multiple Output
MISO	Multiple Input Single Output
ML	Maximum Likelihood
MMSE	Minimum Mean Square Error
MRC	Maximal Ratio Combining
OFDM	Orthogonal Frequency Domain Multiplexing
OFDMA	Orthogonal Frequency Domain Multiple Access
PBCH	Physical Broadcast Channel
PDCCH	Physical Downlink Control Channel
PDSCH	Physical Downlink Shared Channel
PRBs	Physical Resource Blocks
PSS	Primary Synchronization Signals
QAM	Quadrature Amplitude Modulation
QPSK	Quadrature Phase Shift Keying
SC	Select Combining
SFBC	Space Frequency Block Coding
SISO	Single Input Single Output
SNR	Signal to Noise Ratio
SSS	Secondary Synchronization Signals
STBC	Space Time Block coding
STD	Selective Transmit Diversity
TDD	Time Division Duplex
TDTD	Time Division Transmit Diversity
TSTD	Time Switched Transmit Diversity
UE	User Equipment
UMTS	Universal Mobile Terrestrial System
UpPTS	Uplink Pilot Time Slot
Zero Padding	Zero Padding

1. Introduction

1.1 LTE and Channel Estimation

After Universal Mobile Terrestrial System (UMTS) 3G technologies were entertained by many, still the hunger for higher data rate and greater spectral efficiency in wireless environment is ever increasing. This desire necessitated the need for further developments in mobile communication where by Long Term Evolution (LTE) technology is one outgrowth. LTE is an update to the UMTS technology that enables it to provide significantly faster data rates for both uplink and downlink transmissions [1].

As stated in [1] LTE Evolved Packet System (EPS) is purely Internet Protocol (IP) based both in real time services and datacom services. The IP address is allocated throughout the course of communication. The access schemes used in LTE downlink technology is based on Orthogonal Frequency Division Multiple Access (OFDMA) and in combination with higher order modulation (up to 64 QAM) and it has expandable large bandwidths (1.4 up to 20 MHz). In addition in order to achieve higher data rate, spatial multiplexing in the downlink (up to 4x4 MIMO) can be used. The maximum theoretical peak data rate on the transport channel is 75 Mbps in the uplink. And in the downlink, using spatial multiplexing, the rate can be as high as 300 Mbps.

In mobile communication systems the nature of mobile radio channel leads to multipath propagation which results in rapid variations of the phase and amplitude of transmitted signal. This leads to the degradation in the quality of the system unless excellent receiver are implemented that estimate the instantaneous channel variation and take mitigation actions. So channel estimation is an integral part of recent mobile communication systems.

Channel state information (CSI) in wireless communication system provides information on properties of the wireless channel; it takes into account the effect of signal propagation mechanism such as scattering and fading [3]. For reliable communication knowledge of the CSI

is very critical in determining the channel property. Knowledge of CSI can be instantaneous or statistical. In instantaneous CSI, the current channel conditions are known, which can be viewed by knowing the impulse response of the transmitted sequence. In statistical CSI, instead of the current channel condition, a statistical characterization of the channel like fading distribution, channel gain spatial correlation and the like is known [3].

Different channel estimation techniques are introduced in the literature and are broadly categorized as: blind, semi-blind and pilot-aided channel estimations. LTE commonly uses cell-specific reference signals (pilot symbols) inserted in both time and frequency domain in a well-defined configuration to estimate the channel. These inserted pilot symbols provide an estimate of the channel at given locations within a subframe. And by using interpolation, it is possible to estimate the channel across an arbitrary number of subframes [4].

1.2 Statement of the Problem

In the past few years, a number of channel estimation techniques, that are applicable to LTE, are studied. The various techniques were compared using metrics such as computational complexity and performance for various channel variations in time and frequency domains and must be considered in choosing the proper channel estimation technique. Of the compared techniques, pilot assisted channel estimation is the most common techniques used in LTE [5-9].

Comparisons were limited to lower-order modulation orders and focusing on single-input single-output (SISO) with OFDM systems. However, investigating the performance of pilot-based channel estimation techniques at higher order modulations in MIMO-OFDM, to the best of our knowledge, is not addressed. The need for further study to understand the performance of pilot based channel estimations in LTE at higher order modulation schemes that include 16QAM and 64QAM is the motivation of this thesis.

1.3 Objective of the thesis

1.3.1 General Objective

The general objective of this thesis is to evaluate performance of pilot aided channel estimation techniques for LTE downlink with higher-order modulation transmission.

1.3.2 Specific Objectives

The specific objectives for this thesis are to:

- Study LTE system which bases multiple antenna transmission schemes and OFDM.
- Study channel estimation.
- Implement pilot based channel estimation techniques in LTE system.
- Create a simulation platform and investigate the performance of pilot based channel estimation techniques in LTE system in using higher modulation.
- Conclude on the performance of the techniques based on simulation results.

1.4 Significance and Limitation of the Study

The research provides:

- Information on the performance issues of pilot-based channel estimation techniques particularly in the LTE technology.
- For future researchers, it can be used as baseline information in using higher modulation order in estimating the channel for MIMO-OFDM system for LTE downlink system.

The research:

- Is limited to simulation-based investigation which relies on theoretical data.
- Considers only two of the pilot-based channel estimation techniques and LTE downlink system due to time limitation.

1.5 Methodology

In this thesis in order to achieve the objectives,

- Different literature related to this study has been reviewed.
- MATLAB is used to construct the computer code of MIMO transmit diversity mode of LTE downlink system and the simulations were run in MATLAB environment
- Based on simulation results, analysis to compare the performance of channel estimation techniques is done.

1.6 Related Literature review

Here we cite a few references of work done related to channel estimation in LTE wireless networks. [5] evaluates the performance of channel estimation of LS and LMMSE for SISO antenna using QPSK and 16QAM as modulation schemes. It demonstrates performance of LS and LMMSE LTE channel estimators for different interpolation methods such as linear, spline and p-chip and modulation schemes. Simulation results show that, LMMSE's performance for the same channel depends on interpolation method and modulation scheme. However, this paper is limited to SISO antenna.

In [6] deals with the performance analysis of channel estimation methods for LTE downlink system over time varying mobile environments using SISO system. The frequency domain (LS_Freq), least square time domain (LS_Time), maximum likelihood (ML) and minimum mean square error estimation (MMSE) techniques were focus area for different bandwidth by varying the number of resource blocks used in OFDM structure of LTE system. The paper concludes that as number of pilots' increases with increasing bandwidth, performance of the estimator increases. The papers simulations result shows that MMSE performs well at low SNR. LS_Time and ML perform well at high SNR as they use the knowledge of number of channel taps. The simulation is done only for SISO and the methods are not checked for MIMO antenna cases.

[7] introduces and compared the effect of channel length variation on the performance of LS and LMMSE channel estimation techniques for 2x2 MIMO LTE downlink system and QPSK

modulation scheme. The paper's simulations result shows that, in the case where the cyclic prefix is equal to or longer than the channel length, LMMSE performs better than LS estimation but at the cost of computational complexity. In the other case, LMMSE continue to improve its performance only for low signal-to-noise-ratio (SNR) values but it degrades for high SNR values in which LS shows better performance for LTE Downlink systems. In [7] a different approach is used and higher modulation schemes like 16QAM and 64QAM are not covered as a part of the study.

In [8] the channel estimation techniques for OFDM systems based on pilot arrangement are investigated. The channel estimation based on comb type pilot arrangement is studied through different algorithms for both estimating channel at pilot frequencies and interpolating the channel. The estimation of channel at pilot frequencies is based on LS and LMS while the channel interpolation is done using linear interpolation, second order interpolation, low-pass interpolation, spline cubic interpolation, and time domain interpolation and analyses performance of channel estimation techniques under different modulation scheme like 16QAM, QPSK, differential quadrature phase shift keying (DQPSK) and BPSK for SISO and as well in paper [2] for BPSK scheme is performed. The paper is limited to SISO antenna case and further analysis using MIMO antenna is needed.

[9] proposes to evaluate the performance of channel estimation techniques for 2x2 LTE Downlink systems based on Zero Padding technique (ZP) instead of cyclic prefixing (CP) using QPSK modulation scheme. Simulation results have shown that CP-LTE systems outperform ZP-LTE in terms of BER.

The paper [10] proposes to evaluate the channel estimation schemes for LTE downlink based on 3GPP LTE downlink specifications. The results for both SISO and MIMO-OFDM are presented for LMMSE method. First the paper evaluates the SISO–OFDM for QPSK and 16 QAM modulation scheme with LMMSE estimator. Secondly, only QPSK (4-QAM) as a higher modulation schemes and LMMSE channel estimator is used to simulate for 2x2, 2x1 MIMO-OFDM system. The results show that performance of MMSE is superior to LS. However, the

performance gap value between the two algorithms at different modulation scheme i.e., jumping from QPSK to 16QAM is not studied.

Even with the papers just mentioned and work by many other researchers in the past decade, there is less discussion about using MIMO OFDM technology in combination with higher modulations like 16QAM and 64QAM to investigate the performance of channel estimation techniques in LTE environment. This is an open area that needs to be studied more in the future to see the performance of different channel estimation techniques using MIMO OFDM under different modulation scheme and different parameter configuration.

1.7 Outline of the thesis

The organization of the thesis is as follows. Chapter two gives general overview of the LTE system and the OFDM model and the different MIMO modes of transmission used in the LTE system are discussed. Specifically, the MIMO OFDM model i.e., the MIMO 2x2 transmit diversity using Space Frequency Block Coding, which is used in the thesis, is presented.

Chapter three illustrates different channel estimation techniques and the formulations of Least Square and Linear Minimum Square channel estimation algorithms are introduced. Chapter four provide insight into some of the characteristics of the mobile radio channel and different fading channel models. Channel parameters of the wireless environment are given and the different channel models used in the LTE system is provided. In Chapter five performance of Least Square and Linear Minimum Mean Square Estimation techniques at different modulation scheme are evaluated according to the LTE selected parameters and the results are discussed.

Finally, in Chapter six the conclusion based on the results and discussion is presented and some future ideas are given.

2. Overview of LTE System

The motivation of this chapter is to give a detailed description of LTE downlink and LTE system model which bases multiple antenna transmission schemes and OFDM.

2.1 LTE Physical Layer Overview

LTE physical layer is targeted to provide improved radio interface capabilities between the base station and user equipment (UE) compared to previous cellular technologies and in the initial requirements defined by the 3rd Generation Partnership Project (3GPP) (3GPP 25.913), the LTE physical layer should support peak data rates of more than 100 Mb/s over the downlink and 50 Mb/s over the uplink. It has a flexible transmission bandwidth ranging from 1.25 to 20 MHz and will provide support for users with different capabilities. The technology requirement will be implemented will be achieved by employing OFDM or multi-antenna schemes (3GPP 36.201) [14].

Additionally, channel variations in the time/frequency domain are exploited through link adaptation and frequency-domain scheduling, giving a substantial increase in spectral efficiency. In order to support transmission in paired and unpaired spectra, the LTE air interface supports both frequency division duplex (FDD) and time division duplex (TDD) modes [14].

This section discusses a detailed description of the LTE radio-interface physical layer by providing an introduction to the physical layer, focusing on the physical resource structure .And it discuss LTE slot structure, the physical resource elements and LTE downlink parameters.

2.1.1 Physical Resource Structure of LTE

As stated in 3GPP TR 36.211 V8.7.0 document the size of various fields in the time domain for LTE signal is expressed as a number of time units T_s =1/(15000 × 2048) seconds [11]. Downlink

and uplink transmissions are organized into radio frames with T_f = 307200 x T_s =10ms duration. Two radio frame structures are supported: Type-1 frame structure is applicable to Frequency Division Duplex (FDD) and Type-2 frame structure is applicable to Time Division Duplex (TDD).

Type-1 Frame structure

The application of frame structure type 1 is both in full duplex and in half duplex FDD. As shown below in Figure 2.1 the length of each radio frame is 10ms long which is divided into 20 slots of length Ts=15360 x T_s= 0.5ms, numbered from 0 to 19. LTE sub frame consists of two consecutive slots where sub frame i consists of slots 2i and 2i+1.

In using FDD mode, 10 sub frames are used for downlink transmission and 10 sub frames are used for uplink transmissions in each 10ms interval. Uplink and downlink transmissions are separated in the frequency domain. In half-duplex FDD operation, the UE cannot transmit and receive at the same time while there are no such restrictions in full-duplex FDD [11].

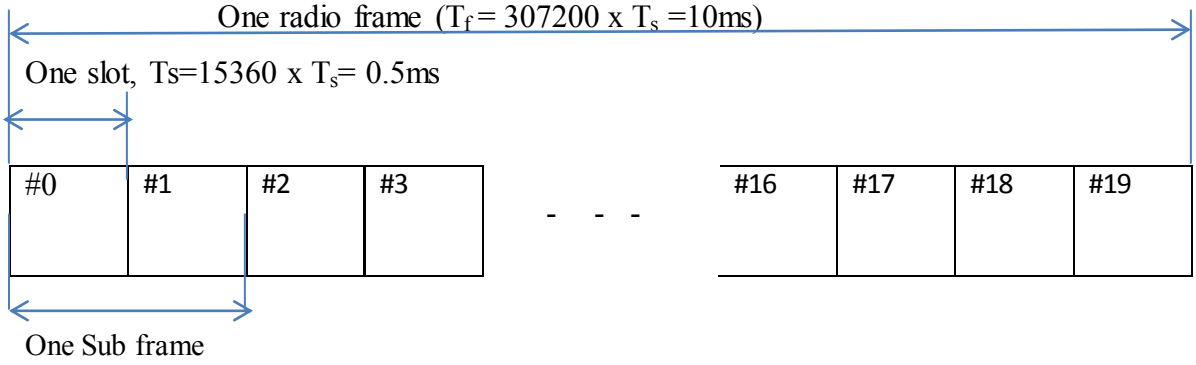

Figure 2.1 Frame structure type 1[11].

Type-2 Frame structure

The application of Frame structure type 2 is in TDD. Each radio frame of length T_f = 10ms consists of two half frame of length 5ms each. Each half-frame consists of five subframes of length 1ms. Table 2.1 lists the supported uplink-downlink configuration where, for each

subframe in a radio frame, 'D' denotes the subframe is reserved for downlink transmissions, 'U' denotes the subframe is reserved for uplink transmissions and 'S' denotes a special subframe with the three fields Downlink Pilot Time Slot (DwPTS), Guard Period (GP) and Uplink Pilot Time Slot (UpPTS). The length of DwPTS and UpPTS is given by Table 2.2 subject to the total length of DwPTS, GP and UpPTS being equal to 1ms. Each subframe i is defined as two slots, 2i and 2i+1 of length T_{slot}=0.5ms in each subframe [11].

Uplink-downlink configurations with both 5ms and 10ms downlink-to-uplink switch-point periodicity are supported. In case of 5ms downlink-to-uplink switch-point periodicity, the special subframe exists in both half-frames. In case of 10ms downlink-to-uplink switch-point periodicity, the special subframe exists in the first half-frame only. Subframes 0 and 5 and DwPTS are always reserved for downlink transmission. UpPTS and the subframe immediately following the special subframe are always reserved for uplink transmission.

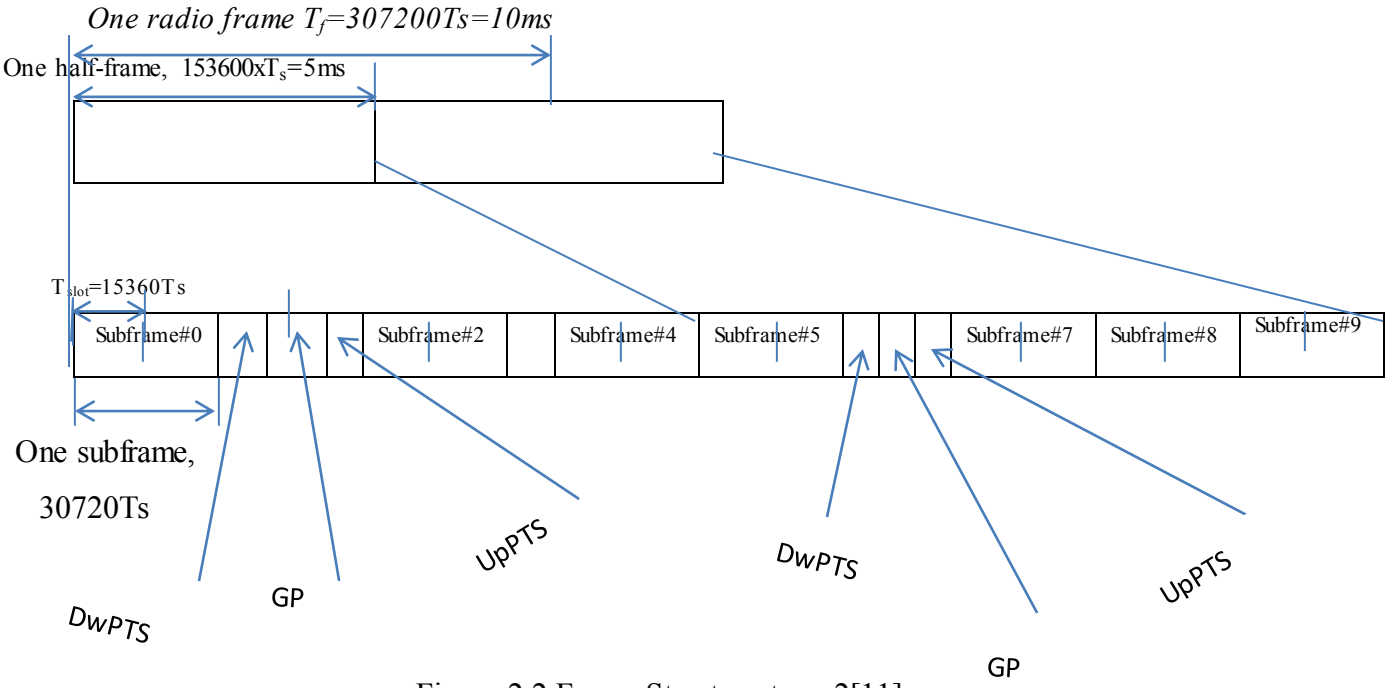

Figure 2.2 Frame Structure type 2[11].

Special subframe configuration	Normal Cyclic prefix in downlink			Extended Cyclic prefix in downlink		
	DwPTS	UpPTS		DwPTS	UpPTS	
		Normal Cyclic prefix in uplink	Extended Cyclic prefix in uplink		Normal Cyclic prefix in uplink	Extended Cyclic prefix in uplink
0	6592.T_s			7680.Ts		
1	19760.T_s			20480.Ts		
2	21952.T_s	2192.Ts	2560.Ts	23040.Ts	2192.Ts	2560.Ts
3	24144.T_s			25600.Ts		
4	26336.T_s			7680.Ts		
5	6592.T_s			20480.Ts	4384.Ts	5120.Ts
6	19760.T_s			23040.Ts		
7	21952.T_s	4384.Ts	5120.Ts	-	-	-
8	24144.T_s			-	-	-

Table 2.1 Configuration of special subframe (lengths of DwPTS/GP/UpPTS)[11].

Uplink-downlink configuration	**Downlink-to-uplink Switch-point Periodicity**	**Subframe number**									
		0	**1**	**2**	**3**	**4**	**5**	**6**	**7**	**8**	**9**
0	5ms	D	S	U	U	U	D	S	U	U	U
1	5ms	D	S	U	U	D	D	S	U	U	D
2	5ms	D	S	U	D	D	D	S	U	D	D
3	10ms	D	S	U	U	U	D	D	D	D	D
4	10ms	D	S	U	U	D	D	D	D	D	D
5	10ms	D	S	U	D	D	D	D	D	D	D
6	5ms	D	S	U	U	U	D	S	U	U	D

Table 2.2 Uplink-downlink configurations [11].

2.1.2 LTE Slot Structure and Physical Resource Elements

Resource grid

As described above the LTE downlink system has 10ms duration for one frame structure. Each frame is divided in to 10 of 1ms sub frames as shown in Figure 2.3. And the sub frame has two time slots of 0.5ms. The slot contains 6 or 7 OFDM symbols based on the number of cyclic prefix added (normal or extended). The LTE downlink system has 25 different frequency bands and scalable bandwidth of 1.4MHz to 20MHz.One physical resource block is 180 KHz and the subcarrier separation is 15 KHz and it is formed by concatenation of resource blocks consisting of 12 sub carriers.

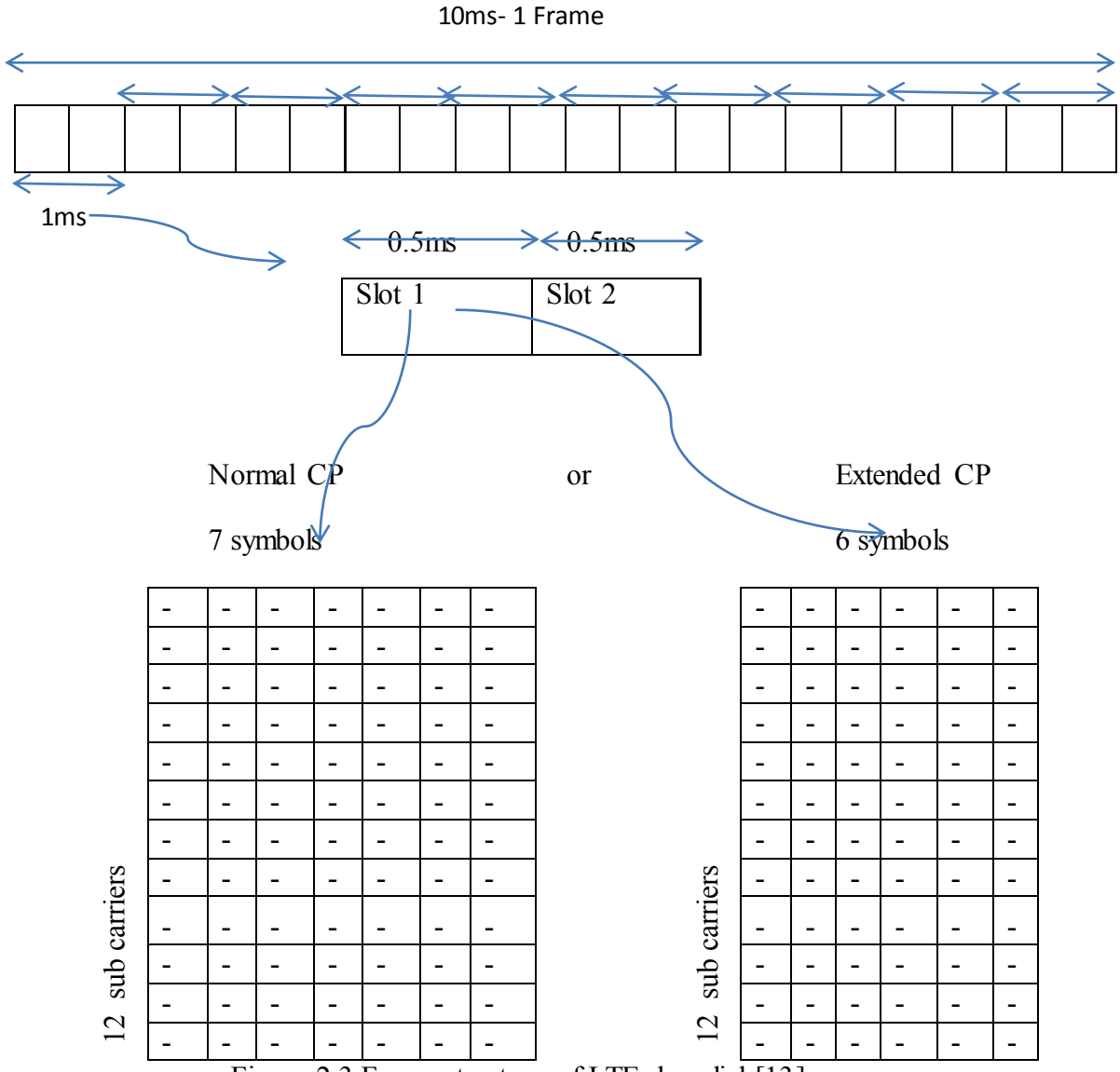

Figure 2.3 Frame structure of LTE downlink[13].

LTE radio resource is structured using units of Physical Resource Blocks (PRBs). The PRB contains 12 subcarriers and one slot to mean that it has 12 by 6 or 7 dimensions. If the normal Cyclic Prefix is used, a PRB will contain 12 subcarriers over seven symbols. If the extended CP is used, the PRB contains only six symbols. The UE is specified allocation for the first slot of a sub frame. For example, in a 10 MHz spectrum bandwidth, there are 600 usable subcarriers (50*12) and 50 PRBs [12, 13]. In general the OFDM parameters are shown in Table 2.3 and the resource grid is shown at Figure 2.4.

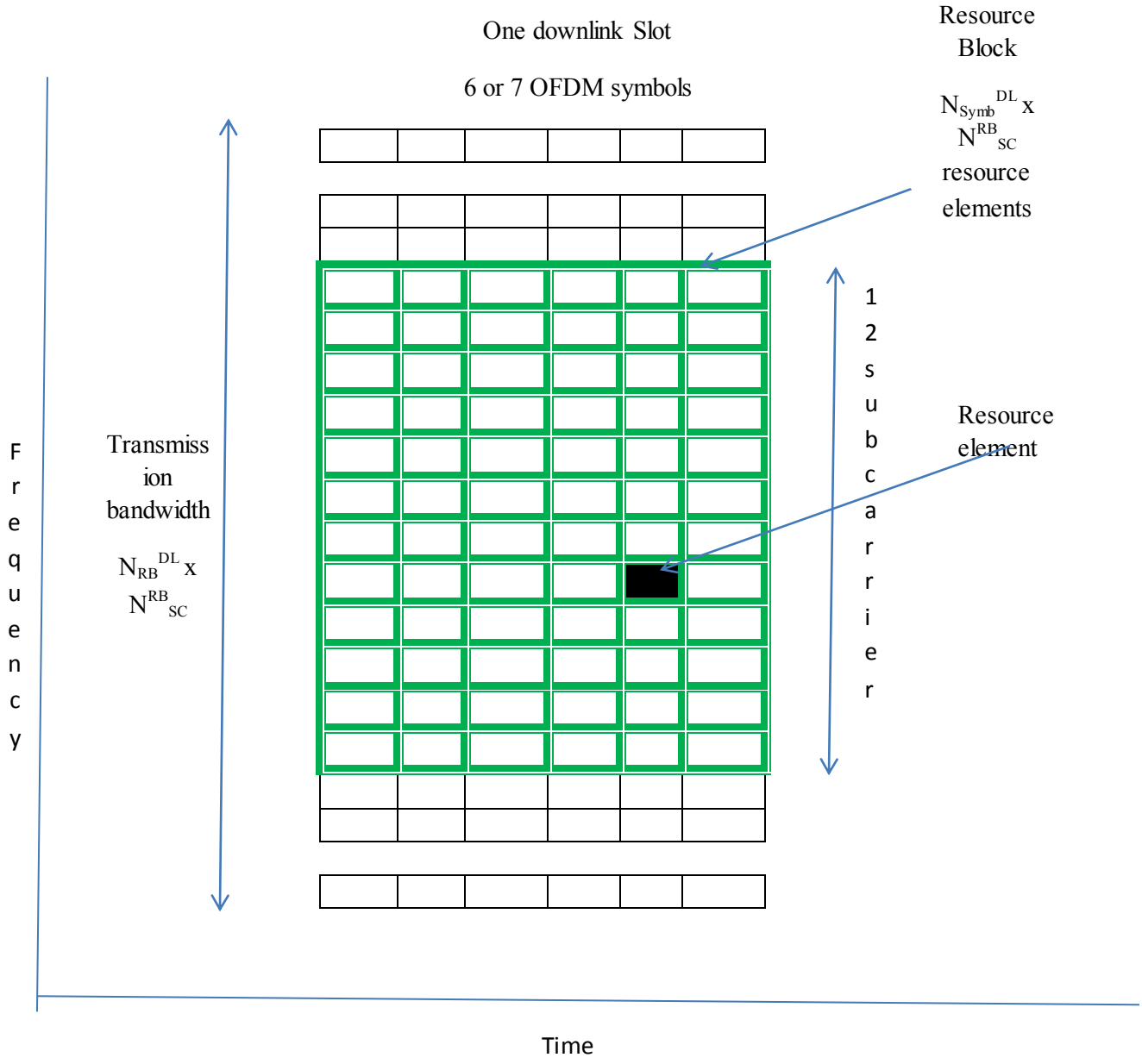

Figure 2.4 LTE Resource grid [6].

2.1.3 LTE Downlink Parameters

Each slot in a transmitted signal resource grid has two dimensions subcarrier ($N^{DL}_{RB}N^{RB}_{SC}$) vs. OFDM symbol(N^{DL}_{Symb}).The transmission bandwidth in the cell determines the quantity N^{DL}_{RB} and it is between 6 and 100. The set of allowed values for N^{DL}_{RB} is listed in Table 2.3.

Band width(MHz)	1.4	3	5	10	15	20
Sampling frequency(MHZ)	1.92	3.84	7.68	15.36	23.04	30.72
FFT size	128	256	512	1024	1536	2048
No. of resource blocks(PRB) N^{DL}_{RB}	6	15	25	50	75	100
OFDM symbols per time slot	7/6 (Normal/Extended)					
CP length(ms)	4.7/5.6 16.67(Normal/Extended)					

Table 2.3 OFDM parameters for LTE downlink system [13].

When we use multi-antenna transmission, each antenna port will have one resource grid. An antenna port is defined by its associated reference signal. The reference signal configuration in the cell will define the set of antenna ports [11]:

- Cell-specific reference signals, associated with non-Multicast Broadcast Single Frequency Network (non-MBSFN) transmission, support a configuration of one, two, or four antenna ports and the antenna port number p shall fulfill p=0, p∈ {0,1} and p∈ {0,1,2,3} respectively.
- MBSFN reference signals, associated with MBSFN transmission, are transmitted on antenna port p=4.
- User Equipment (UE)-specific reference signals are transmitted on antenna port p=5.

2.1.4 Downlink Reference Signals

Coherent demodulation at the user equipment is possible using channel estimation based on pilot symbols (reference symbols) that are inserted in OFDM time-frequency grid. In the case of one antenna, LTE system has a special configuration of inserting the pilot symbols in a such a way that the downlink pilot symbols are inserted at the first and third last OFDM symbol of each slot with a frequency domain spacing of six sub-carriers and there is a frequency domain gap of three sub-carriers between the first and second reference symbols [14]. As a result of this each resource block will allow four pilot symbols.

When there are two antennas used in the transmitting side of the LTE system, pilot symbols orientation of the two antenna ports is different from that of the one antenna port transmission. In this case pilot symbols are inserted from each antenna where the pilot symbols on the second antenna are offset in the frequency domain by three subcarriers. To maximize accurate estimation of channel coefficients, there is nothing transmitted on the other antenna at the same time-frequency location of pilot signals to mean that resource element carrying the reference signal for an antenna; the corresponding resource elements in other antennas have null transmissions. This allows the pilot signals to transmit without interference from the other antenna transmissions. The following Figures, Figure 2.5 and Figure 2.6 illustrate the concepts that are described above.

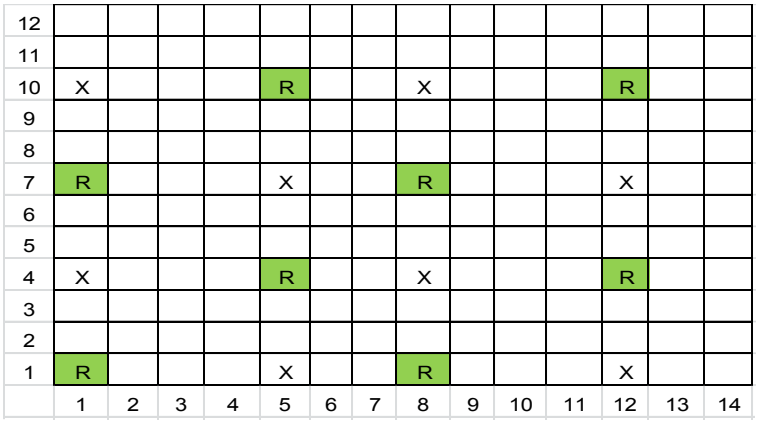

Figure 2.5 One antenna system pilot symbol arrangements for LTE downlink system [14].

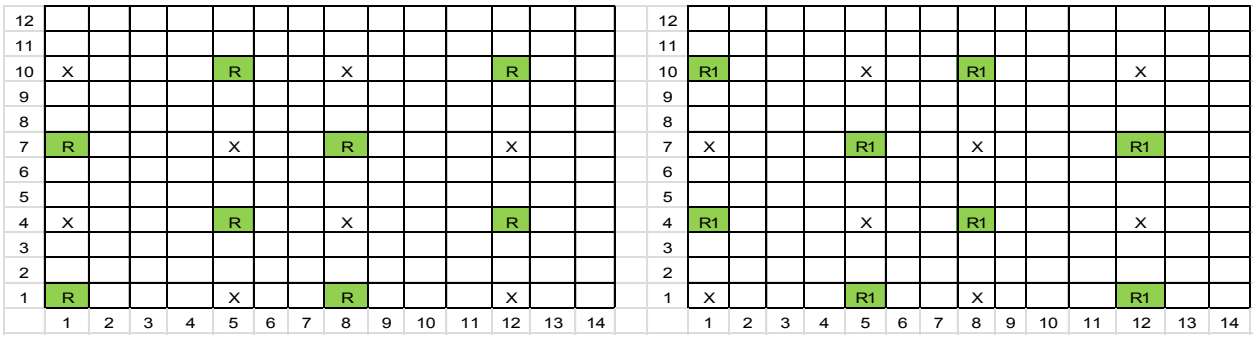

Figure 2.6 Two port antenna pilot arrangement for LTE downlink system [14].

For Four antenna port configuration case, a different pilot arrangement is used. The pilot symbol position and cell identity determine the values of the pilot symbols which is complex value. In LTE system, there are 510 reference signal sequences which correspond to 510 different cell identities.

2.2 LTE System Model

LTE system model[1] is based on Orthogonal Frequency Division Multiple Access (OFDMA) as multiple access method and in combination with higher order modulation, with large bandwidths and spatial multiplexing or transmit diversity in the downlink using MIMO antennas in order to achieve a high data rates or an improvement in the received signal quality.

When we are using multi-antenna transmission schemes, it maps the modulated data symbols to multiple antennas ports. Using OFDM transmission scheme, the resource grid is constructed in each antenna; OFDM symbols are generated, and transmits the signal. In a MIMO–OFDM system, the process of resource-grid mapping and OFDM modulation is repeated over multiple transmit antennas. The basic idea of OFDM is using a multi-carrier transmission [13].

2.2.1 Multi-carrier Transmission

Multi-carrier transmission is one of the ways to increase the overall transmission bandwidth, without suffering from increased signal corruption due to radio-channel frequency selectivity. As shown in Figure 2.7 in multi-carrier transmission multiple narrowband signals, also called as

subcarriers, are transmitted instead of a single wideband signal. The subcarriers are frequency multiplexed and jointly transmitted over the same radio link to the same receiver. Parallel transmission of N signals over the same radio link can help to achieve an N times increase in the overall data rate.

In addition, the effect of signal corruption as a result of radio-channel frequency selectivity only depends on the bandwidth of each subcarrier. As a result, the impact from a frequency-selective channel is basically the same as for a more narrowband transmission scheme with a bandwidth that corresponds to the bandwidth of each subcarrier [4].

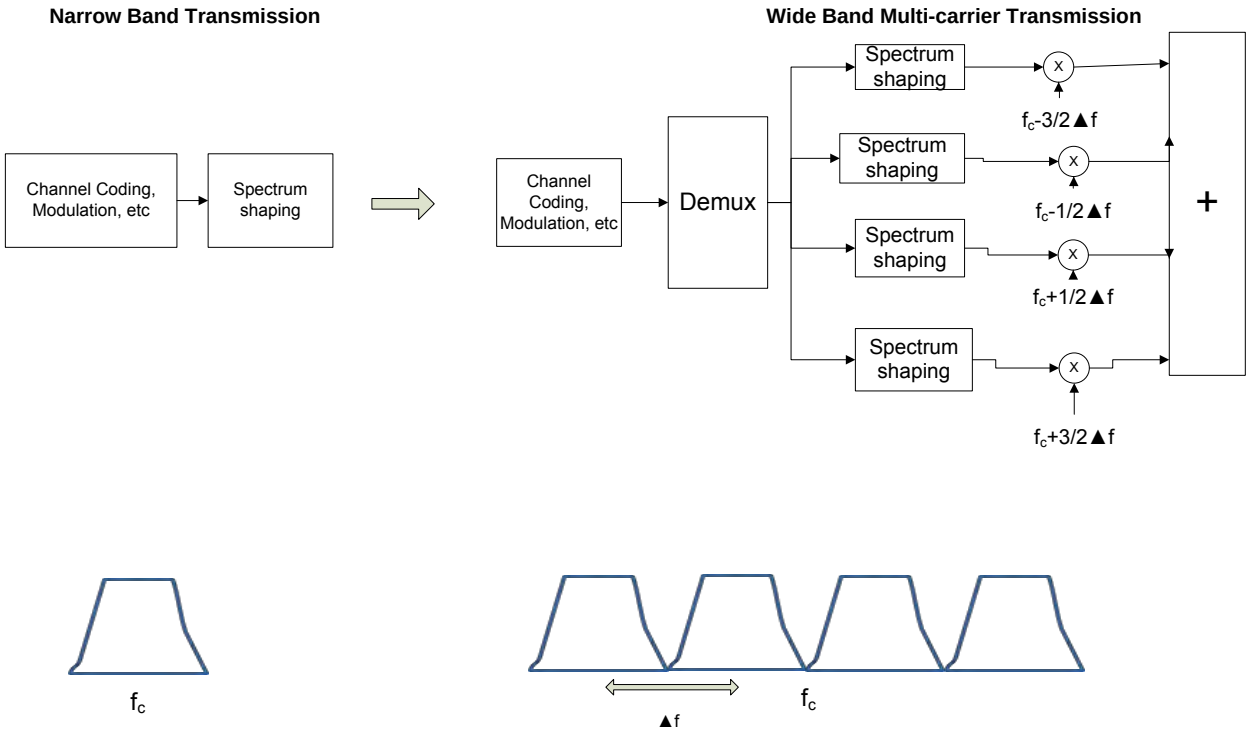

Figure 2.7 Extension to wider transmission bandwidth by means of multi-carrier transmission[4].

The problem of multi-carrier evolution outlined in Figure 2.7 is that extending the narrow band radio access technology to a wider overall transmission by making parallel transmission of N more narrow band carriers, there is a problem of making spectrum packing and there will be some gap or valley in the overall transmission and this has a negative impact in overall bandwidth efficiency.

In addition to the above problem multi-carrier transmission using parallel transmission of multiple carriers results in larger variations in the instantaneous transmit power. As a result the method has negative effect on the transmitter power-amplifier efficiency, to mean that increased transmitter power consumption and increased power-amplifier cost. Alternatively, we reduce the average transmit power. Due to this reason the use of multicarrier transmission is more appropriate for the downlink transmission than the uplink transmission.

OFDM techniques can be used as a method to implement a multi-carrier modulation which is a different approach and will be discussed in the next section.

2.2.2 Orthogonal Frequency Division Multiplexing

OFDM transmission scheme is a type of a multichannel system where it uses multiple subcarriers. To increase the bandwidth efficiency the spectrums of subcarriers are made overlapping and the wideband is fully divided into N orthogonal narrowband sub channels. These orthogonal signals are created using Discrete Fourier Transform (DFT) and Inverse DFT (IDFT) processes. DFT and IDFT can be implemented efficiently by using fast Fourier transform (FFT) and inverse fast Fourier transform (IFFT), respectively [15]. LTE uses OFDM as a basic scheme as it is illustrated in Figure 2.8.

In LTE downlink system the input data stream is modulated by either of QPSK, 16 QAM or 64 QAM modulator and this results in a complex symbol stream [16]. The modulated symbol are passed through a serial-to-parallel converter, and results a set of N parallel QPSK ,16QAM or 64QAM symbols corresponding to the symbols transmitted over each of the subcarriers. Thus, the N symbols output from the serial-to-parallel converter are the discrete frequency components of the OFDM modulator output. The use of the IDFT and DFT are used for modulating and demodulating the data constellations on the orthogonal sub-carriers respectively [17, 19].

Cyclic prefix as a guard interval (GI) is used in the model and its length should exceed the maximum excess delay of the multipath propagation channel is a basic principle [18]. Due to the cyclic prefix, the transmitted signal becomes “periodic”, and the effect of the time-dispersive

multipath channel becomes equivalent to a cyclic convolution, discarding the guard interval at the receiver.

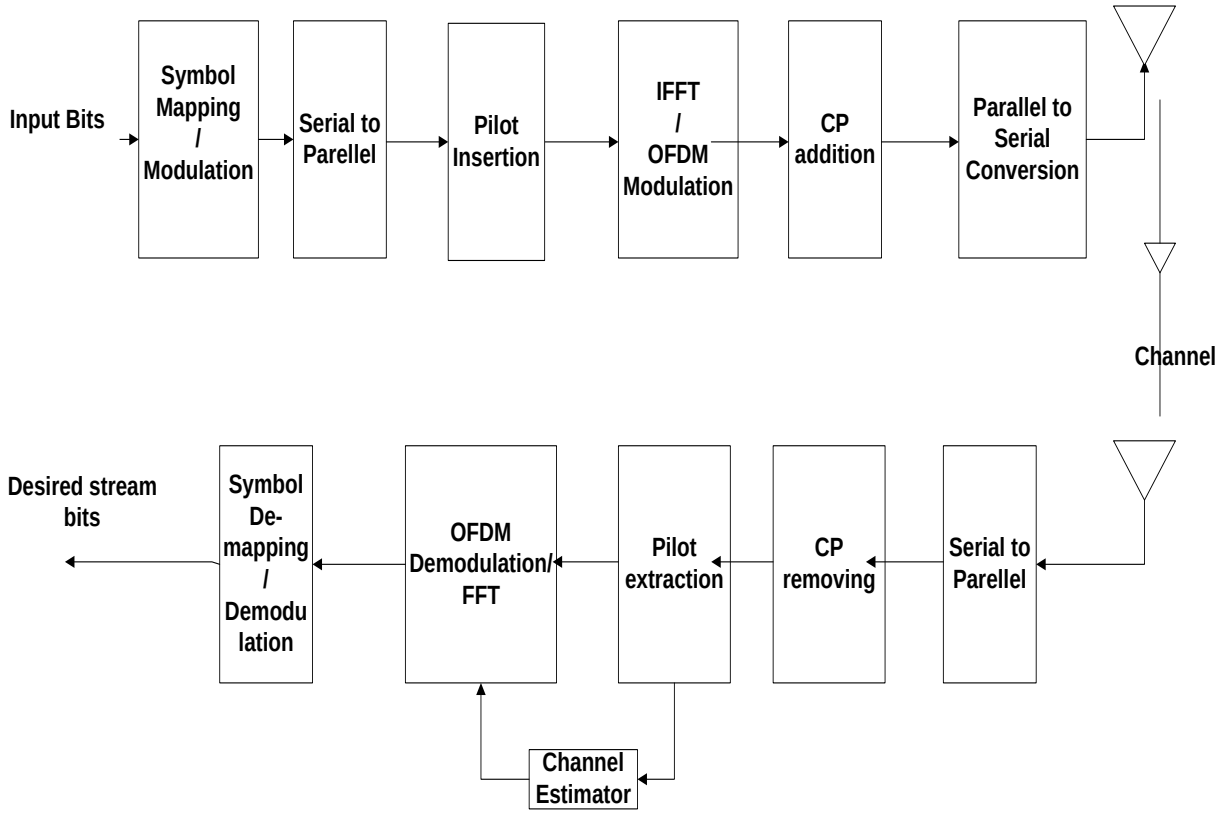

Figure 2.8 A simplified OFDM Model [15].

2.2.3 Multiple Input Multiple Output

In theory, data rates in wireless communications can be increased by increasing the overall received signal power for a given transmit power [4]. The use of multiple antennas at the transmitter and/or the receiver can increase the received power. This technique of using multiple antennas is called MIMO technique. The Multi-antenna or MIMO technique is helpful to achieve improved system performance, increase system capacity and increase coverage; in addition it improves service provisioning (higher per-user data rates). The use of MIMO has been the subject of new developments in the area of wireless technology in the past decade [4].

At it is illustrated in the Figure 2.9 the MIMO system has M transmit and N receive antennas. By transmitting through the same channel, every antenna receives not only the direct components intended for it, but also the indirect components intended for the other antennas. The transmission matrix that is obtained from MIMO system H has a dimension of N x M [20].

$$H=\begin{bmatrix} h_{11} & h_{21} & \dots & h_{n1} \\ h_{12} & h_{22} & \dots & h_{n2} \\ \vdots & \vdots & \dots & \vdots \\ h_{1m} & h_{2m} & \dots & h_{nm} \end{bmatrix} \quad \dots\dots\dots\dots\dots\dots\dots\dots (2.1)$$

Considering the noise n, the following transmission formula is formulated from receive antenna vector y, transmit antenna vector x.

$$y = Hx + n \quad \dots\dots\dots\dots\dots\dots\dots\dots (2.2)$$

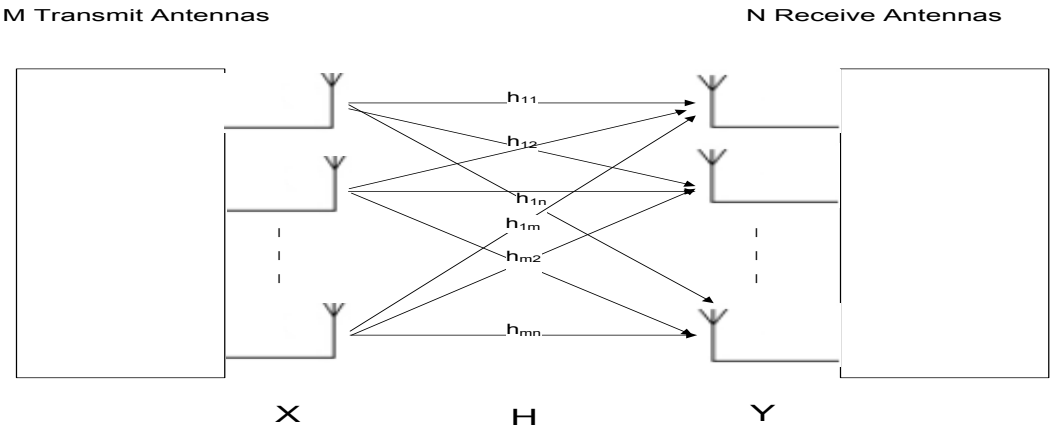

Figure 2.9 MIMO System [20].

LTE uses the advantage of MIMO techniques by introducing many forms of multi-antenna technique in the different transmission modes. The MIMO techniques used in the LTE standard, in general, can be subdivided into three categories: spatial diversity, beam forming, and spatial-multiplexing and each of them are explained below.

2.2.3.1 Spatial Diversity

In wireless communication systems data is transmitted over a radio channels whose time-varying behavior causes severe variations of the amplitude of the received signal. Multipath transmission, Doppler spread, and shadowing nature of the wireless environment can result in variation of received power, called *fading* [16]. Diversity techniques exploit the random nature of radio propagation by finding independent uncorrelated signal paths by transmitting multiple times redundant information; this can improve the wireless communication in the fading environments. The purpose of spatial diversity is by providing the receiver with multiple uncorrelated replicas of the same information bearing signal to combat the effect the different fading problems in the radio channel. Doing so, however, does not increase the data rate. Duplicate date with over different paths are sent and received to increase the robustness of the received signal. The spatial diversity can be further categories as transmitting diversity, receive diversity or cyclic delay diversity.

2.2.3.1.1 Receive Diversity

Receive diversity uses more than one antennas on the receiver side. The simplest scenario consists of two RX and one TX antenna as shown in Figure 2.10

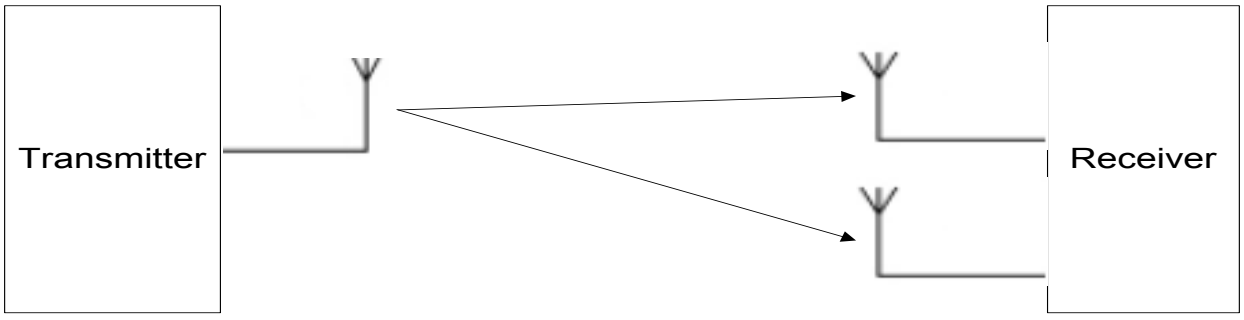

Figure 2.10 Receive diversity [20].

Receive diversity is the most common and simple to implement diversity technique. In receive diversity techniques, the diversity gain can be improved by keeping a sufficient spacing between the multiple antennas at the receive side which reduce the mutual correlation between the antennas. At the receiver the received signals from multiple antennas is combined to get the

diversity gain. And the main combining methods are, select combining (SC), maximal-ratio combining (MRC), equal gain combining (EGC), and square-law combining [14].

2.2.3.1.2 Transmit Diversity

Using multiple transmit antennas, transmit diversity provides the receiver with different path of multiple uncorrelated replicas of the same signal. Transmit diversity reduces the receiver complexity and improve the detection performance [14, 4]. The advantage here is that the complexity of having multiple antennas is placed on the transmitter rather than on mobile station (receiver) side which may be shared among many receivers. The detection performance improvement is possible by having a low mutual correlation between the paths of the different antennas and this can be achieved by means of a sufficiently large distance between the antennas, or by the use of different antenna polarization directions. In order to realize transmitter diversity different approaches can be taken, differentiated by the method of using the multiple transmit antennas.

Transmit diversity is straight forward for systems that use time division duplexing (TDD), where different time slots on the same carrier are used in the forward and reverse link transmission. For TDD systems, the channel impulse response satisfies the reciprocity principle [22]. At the base station the signals received on all antennas can be processed during every received burst. During the next forward burst, the antenna that provided the highest received symbol energy-to-noise ratio is selected and used. This is a form of selective transmit diversity (STD). Obviously, this scheme requires that the channel change slowly. For frequency division duplexed (FDD) systems, transmit diversity is more complicated to implement, because the forward and reverse links are not reciprocal. Time division transmit diversity (TDTD) can be used for FDD by switching the transmitted signal between two or more transmit antennas. Alternate bursts are transmitted through two or more separate antennas, a technique known as time switched transmit diversity (TSTD) [14]. Different approaches can be taken to realize the diversity offered by the multiple transmit antennas. One form is the delay diversity which is discussed below in the next section.

Delay Transmit Diversity

Delay transmitter Diversity is a method where copies of the same data are transmitted through multiple antennas at different times to create artificial delay spread so the resulting channel looks like a fading inter Symbol Interference (ISI) channel. The availability of multiple transmit antennas can be used to create artificial time dispersion or, equivalently, artificial frequency selectivity by transmitting identical signals with different relative delays from the different antennas as shown in Figure 2.11 when the channel in itself is not time dispersive. These results in the antenna diversity since the fading experience by the different antennas has low mutual correlation can be transformed into frequency diversity [4]. There is a special form of delay diversity called cyclic delay diversity and it is described in the next section.

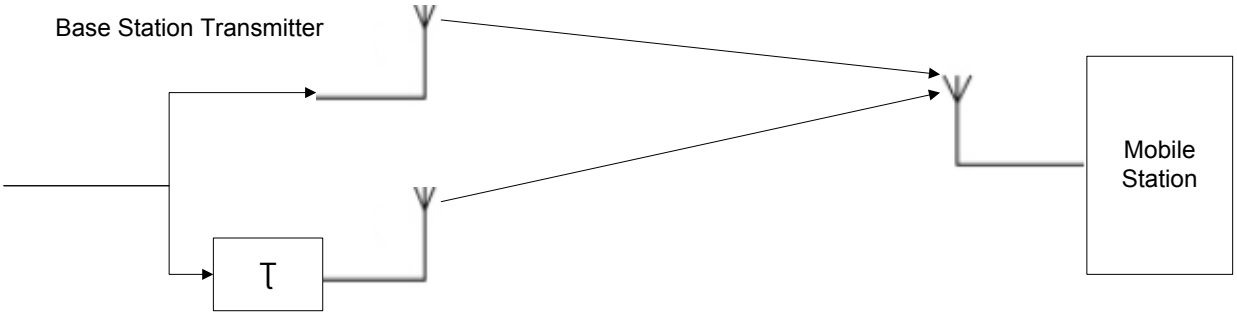

Figure 2.11 Delay diversity [4].

Cyclic Delay Diversity

Cyclic-delay diversity (CDD) differ from the above delay diversity is that it operates block-wise and applies cyclic shifts, rather than linear delays, to the different antennas as it is shown in Figure 2.12 (a). Due to this reason the application of cyclic-delay diversity is block based transmission schemes like OFDM.

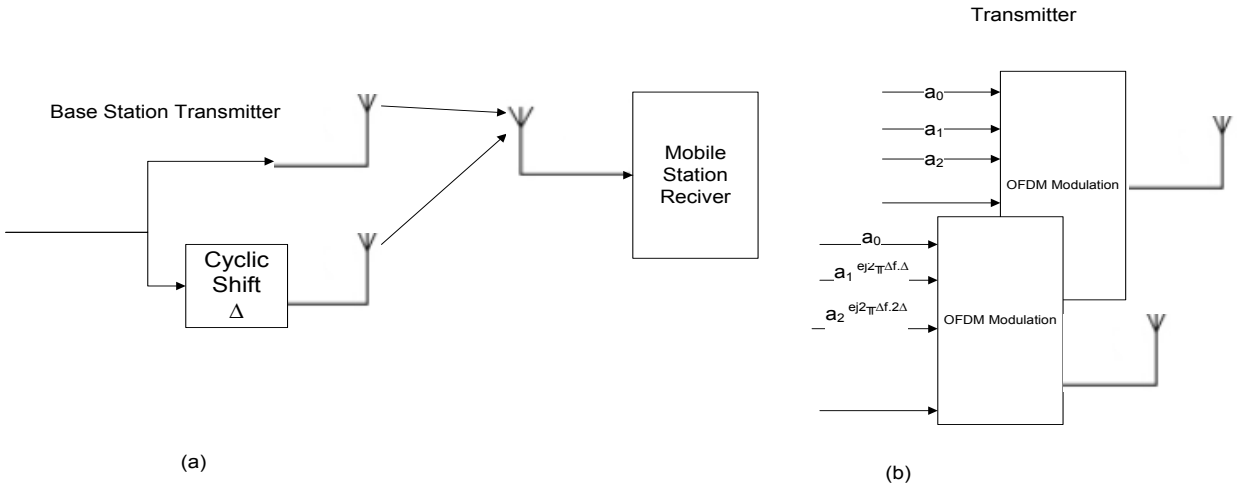

Figure 2.12 Cyclic delay diversity [4].

For OFDM transmission a cyclic shift of the time-domain signal corresponds to a frequency-dependent phase shift is used to create artificial frequency selectivity as seen by the receiver before OFDM modulation, as illustrated in Figure 2.12 (b). The method is expandable to more than two more than two transmit antennas with different cyclic shifts for each antenna.

Other forms of transmit diversity use space-time or space-frequency encoding to come up for diversity gain. When modulation symbols are mapped in the time and spatial (transmit-antenna) domain to capture the diversity offered by the multiple transmit antennas, we call it space time coding in the multi antenna transmission scheme [4].

These forms require three functions:

a. The encoding process using encoders and transmitting of the information sequence
b. The combining scheme using combiner at the receiver,
c. The decision making

Alamouti [22] has developed a method of simple repetition transmit diversity scheme with maximum likelihood combining at the receiver side. By using two transmit antennas and one receiver antenna, using the proposed scheme one can achieve the same diversity order as maximal ratio receiver combining with one transmit antenna and two receiver antennas. This method requires no feedback from the receiver to the transmitter, and requires no bandwidth

expansion. However, to estimate the channel, the scheme requires separate pilot sequence insertion and extraction for each of the transmit diversity antennas [21].

Space-time Block Coding (STBC) with two antennas has been part of the 3G WCDMA standard and can be regarded as a multi-antenna modulation and mapping technique that provides full diversity and results in simple encoders and decoders. Alamouti code is the simplest forms of STBC [a simple transmit diversity] which is defined for a two-antenna transmission. In STBC with Alamouti code, as illustrated in Figure 2.13, pairs of modulated symbols (S_1, S_2) are mapped on the first and second antenna ports in the initial sample time meaning that the modulation symbols are directly transmitted on the first antenna. In the next sample time, the symbols are swapped and further more sign reversed and conjugated ($-S_2^*$, S_1^*) and mapped to the first and second antenna ports and the resulting two consecutive vectors in time are orthogonal.

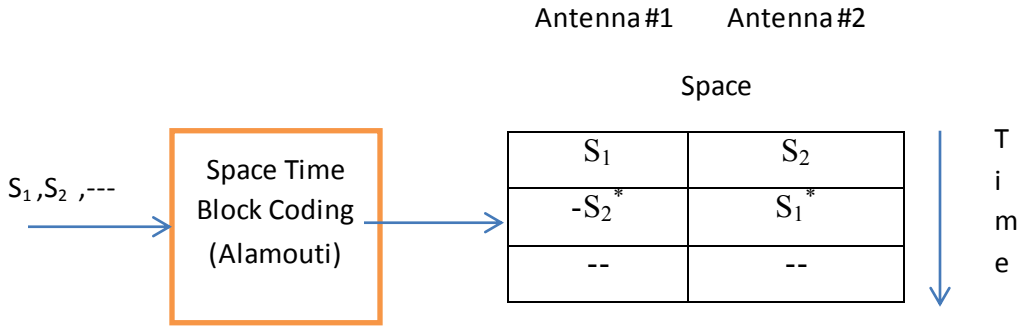

Figure 2.13 Space Time block coding [4].

As LTE use the Space frequency block coding (SFBC) scheme to get transmit diversity gain, the following section illustrates the SFBC scheme.

2.2.3.1.3 Space Frequency Block Coding

From three mode of transmission in LTE, transmit diversity is the second mode of transmission which is based on Space Frequency Block Coding (SFBC) and Frequency Switched Transmit Diversity (FSTD) for two- and four-antenna transmission, respectively. When compared to single-antenna transmissions, both methods offer increased performance using their diversity.

SFBC is a method of transmit diversity which is closely related to Space time block coding(STBC) that is developed by Alamouti [22] and it is selected as the transmit diversity method in the LTE standard when two port antenna is used. The main difference between the two techniques is that in SFBC the encoding is done in the antenna (space) and frequency domains rather than in the antenna (space) and time domains, as is the case for Space Time Block Coding (STBC) [13].

As it is illustrated in Figure 2.14 in SFBC pairs of consecutive modulated symbols (S_1, S_2) mapped directly on to consecutive samples in time on the first antenna port. On the second port, the swapped and transformed symbols ($-S_2^*$, S_1^*) are mapped consecutively in time such that the consecutive vectors on different antennas are orthogonal. We can produce the SFBC output symbols through a simple transformation followed by STBC using the Alamouti code [23, 13].

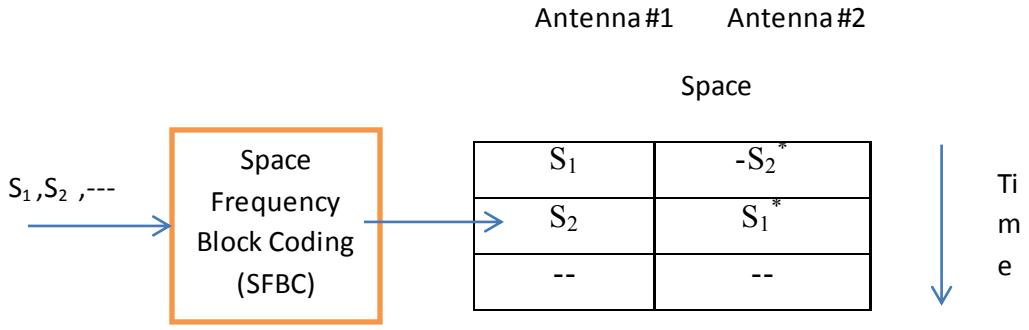

Figure 2.14 Space Frequency block coding [4].

In OFDM, the block of (frequency-domain) modulation symbols S_1, S_2, S_3, S_4, … is directly mapped to OFDM carriers of the first antenna, on the other hand the block of symbols $-S_2^*$, S_1^*,$-S_4^*$,S_3^*, … is mapped to the corresponding subcarriers of the second antenna.

A MIMO operation specified in the LTE standard contains a combination of layer mapping and pre-coding and these two processes combined as encoding operation in the transmit-diversity mode of transmission. The transmit-diversity encoder subdivides the modulated symbols into pairs and through diversity coding places transformed versions of modulated pairs on different transmit antennas. As the samples on each transmit antenna are derived from the original

modulated stream, layer mapping is also implicit and pre-coding can be considered the result of various conjugations and negations. For the Four antennas port LTE configuration a different approach called Frequency Switched Transmit Diversity (FSTD) in combination with SFBC is used.

2.2.3.2 Spatial Multiplexing

In spatial multiplexing mode of transmission, the system transmits different (not redundant) data on different antennas in the contrary to transmit diversity mode of transmission. The data rate of a given communications link is boosted by this mode of MIMO as the data rate can increase linearly in proportion to the number of transmit antennas. The ability to transmit independent data streams in spatial multiplexing comes with a cost, however. Spatial multiplexing is susceptible to deficiencies in rank of the matrix representing the MIMO equation. Multiple techniques are introduced in LTE spatial multiplexing in order to minimize the probability of these rank deficiencies occurring and to harness its benefits [13].

There are two classes of spatial multiplexing open loop spatial multiplexing and closed loop spatial multiplexing. No pre-coding matrix feedback is employed in open loop spatial multiplexing, whereas in closed loop spatial multiplexing, the optimum pre-coding matrix information is feedback by the user equipment (UE) to the evolved node B (eNodeB) [45].

In spatial multiplexing scheme, the process can be described by three parameters: transmit vector X, pre-coding matrix W and output vector Y. thus,

$$y = Wx \qquad \text{..... (2.3)}$$

Open loop spatial multiplexing with CDD

In order to achieve higher data rates, this mode supports spatial multiplexing of two to four layers that are multiplexed to two to four antennas, respectively. Regarding the channel situation, it requires less UE feedback (no pre-coding matrix indicator is included), and is used when

channel information is missing or when the channel rapidly changes, like for UEs moving with high velocity. The signal is supplied to every antenna with a specific delay (cyclic delay diversity, or CDD), thus artificially creating frequency diversity as shown in Figure 2.15 [46].

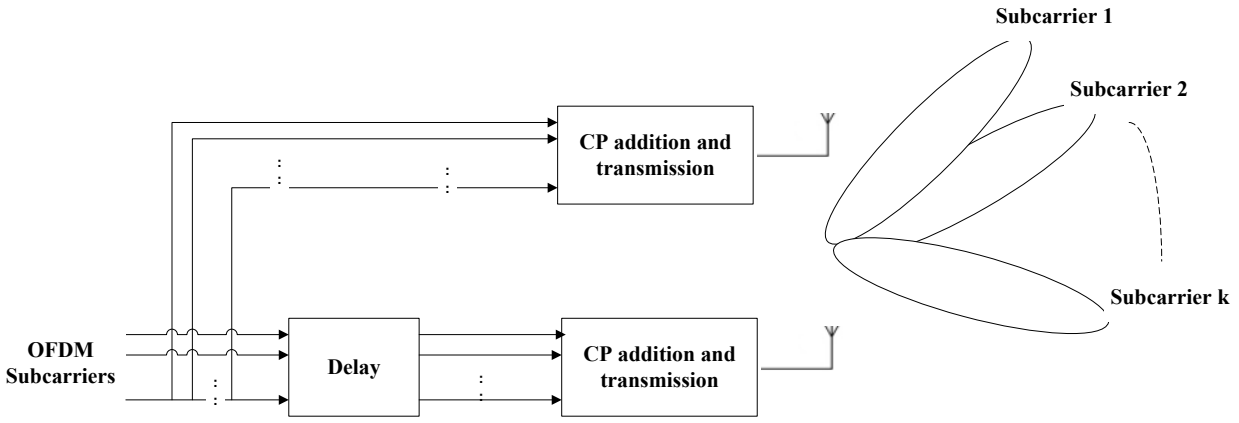

Figure 2.15 Spatial multiplexing with CDD; the individual subcarriers are delayed artificially [46].

Closed loop spatial multiplexing

To achieve higher data rates, closed loop spatial multiplexing supports multiplexing with up to four layers that are multiplexed to up to four antennas, respectively. The base station transmits cell-specific reference signals (CRS), distributed over various resource elements and over various timeslots to permit channel estimation at the receiver. A response regarding the channel situation is sent by UE, which includes information about which pre-coding is preferred from the defined codebook. An index (pre-coding matrix indicators) defined in the codebook; a table with possible pre-coding matrices that is known to both sides is used to accomplish this [46].

2.2.3.3 Beam forming

Beam forming MIMO technique is the shaping of overall antenna beam in the direction of the intended receiver terminal and this is done by using the available knowledge of the downlink channels(the relative channel phases) of the different transmit antennas at the transmitter side. Beam forming technique increases the signal strength at the receiver in a factor proportion to the number of transmit antennas [4].

This mode in LTE uses UE-specific reference signals. Using the same antenna weightings both the data and the reference signals are transmitted. The data transmission for the UE appears to have been received from only one transmit antenna, because the UE requires only the UE specific reference signals for demodulation of the PDSCH, and the UE does not see the actual number of transmit antennas. Therefore, this transmission mode is also called "single antenna port: port 5". The transmission appears to be transmitted from a single "virtual" antenna port 5 [46].

3. Channel Estimation

This chapter discusses the different channel estimation techniques and most of the discussion focuses on pilot-based channel estimation techniques since it is selected for this thesis. Little is discussed on blind and semi-blind channel estimation.

Wideband wireless radio communication channel is time varying and frequency selective. At the receiving end the information bits are retrieved accurately, if the channel characteristics are fully known. The channel may vary instantaneously because of the propagating medium, which leads to the signal degradation. The effect of the medium on the transmitted data has to be characterized or analyzed with a method called channel estimation. This estimation technique has the advantage of getting the channel state information which is pointed out in the introduction chapter. Having the knowledge of CSI is used to describe how the signal propagates from the transmitter to the receiver by having the effect of fading, scattering, attenuation and different channel parameters. Channel estimation techniques allow the receiver to take into account the effect of channel on the transmitted signal and compensate it accordingly which is a very important factor for reliable communication [24].

In general, the basic classifications of channel estimation are three namely pilot based, semi blind and blind channel estimations. A training (pilot) based channel estimation uses a preamble or pilot symbols known to both transmitter and receiver and employ various interpolation techniques to estimate the channel response of the subcarriers between pilot tones. Blind channel estimation is done by evaluating the statistical information of the channel and particular properties of the transmitted signals. Finally semi blind channel estimation is a combination of the two [24].

3.1 Pilot-based Channel Estimation

3.1.1 Pilot Structure

In OFDM systems channel estimation is generally performed by using pilot subcarriers in given positions of the frequency-time grid. The estimation in this system is chosen by taking into account the required performance, computational complexity and time-variation of the channel. Based on the arrangement of pilots placed in the OFDM structure, three different types of pilot structures are considered: block type, comb type, and lattice type [27-30]. According to 3GPP, LTE has special configuration of the pilot insertion in the OFDM structure according to number of antennas used as described in Chapter two which is used in this thesis.

3.1.1.1 Block Type arrangement

As shown in Figure 3.1 pilots are placed for a block type of pilot arrangement. As it shown OFDM pilot symbols at all subcarriers are transmitted in a certain period for channel estimation. A time domain interpolation using the pilots is performed to estimate the channel along the time axis. As explained in [15] denoting S_t for the period of pilot symbols in time to combat time varying channel characteristics, the pilot symbols must be placed as frequently as the coherence time is.

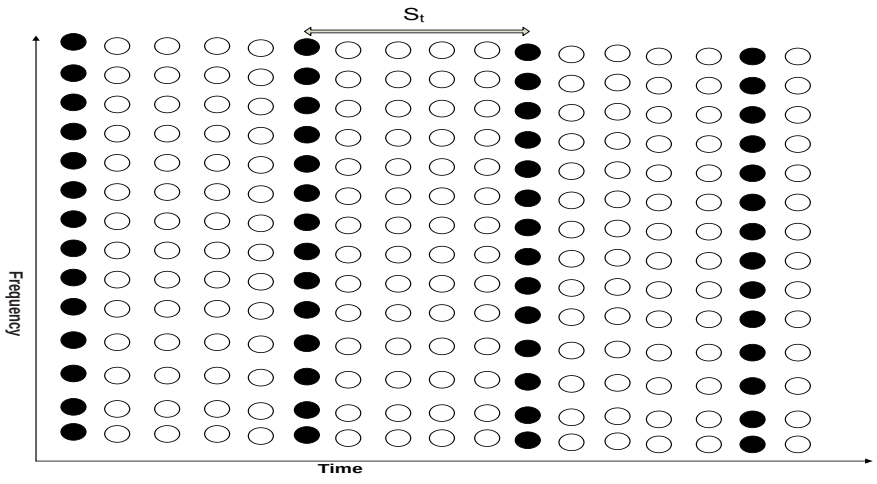

Figure 3.1 Block type OFDM pilot arrangement [15].

The coherence time is given in an inverse form of the Doppler frequency $f_{Doppler}$ in the channel and the pilot symbol period must satisfy the following inequality:

$$S_t \leq \frac{1}{f_{Doppler}} \qquad \text{..... (3.1)}$$

The block-type pilot arrangement is suitable for frequency-selective channels because pilot tones are inserted into all subcarriers of pilot symbols with a period in time. For the fast-fading channels, however, it might incur too much overhead to track the channel variation by reducing the pilot symbol period.

3.1.1.2 Comb Type Arrangement

As shown in Figure 3.2 instead of all subcarrier the pilots are placed at periodically located subcarriers which are used to perform frequency domain interpolation to estimate the channel along the frequency axis.

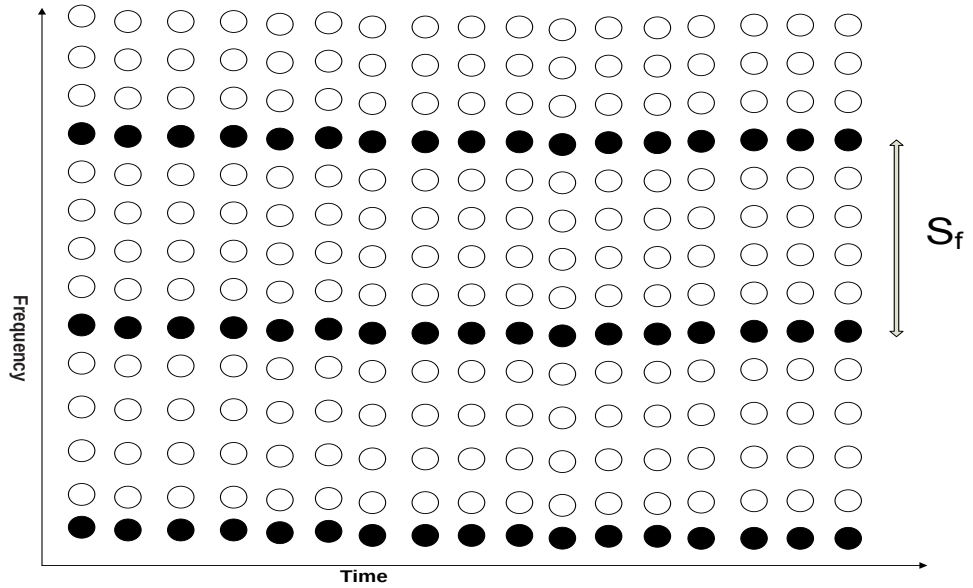

Figure 3.2 Comb type pilot arrangement [15].

Denoting S_f the period of pilot of tones in frequency, the pilot symbols must be placed as frequently as coherent bandwidths in order to track the frequency-selective channel

characteristics. The coherence bandwidth is calculated by an inverse of maximum delay spread $\boldsymbol{\sigma_{max}}$ with the following inequality [15].

$$S_f \leq \frac{1}{\boldsymbol{\sigma_{max}}} \qquad \text{..... (3.2)}$$

In contrary to the block-type pilot arrangement, the comb-type pilot arrangement is suitable for fast-fading channels, but not for frequency-selective channels.

3.1.1.3 Lattice Type Arrangement

In this type pilot arrangement the pilots are inserted along both in time and frequency axes with certain frequency as shown in Figure 3.3. For channel estimation this arrangement can facilitate interpolation of time/frequency domain.

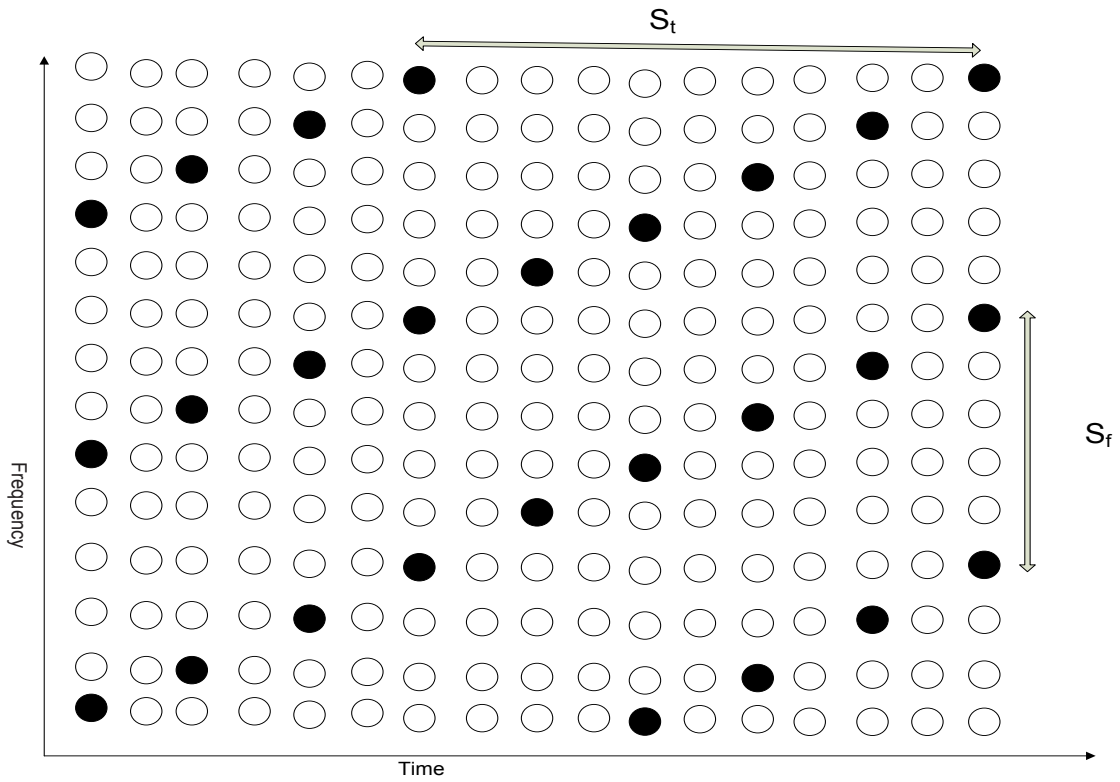

Figure 3.3 Lattice type pilot arrangement [15].

To keep track of both time-varying and frequency-selective channel characteristics, the pilot symbol arrangement must satisfy both inequalities in Equation 3.1 and 3.2 [15].

$$S_t \leq \frac{1}{\text{f Doppler}} \text{ and } S_f \leq \frac{1}{\sigma max} \quad \text{..... (3.3)}$$

3.1.1.4 LTE Pilot Arrangement

As explained in Chapter two in LTE downlink system, the cell specific downlink reference signals are transmitted on one or more antenna ports of the eNodeB for facilitation of the demodulation of the OFDMA signal at the UE. It has special pilot arrangement according to the specification of 3GPP [14].

In using MIMO transmission, a special type of the time-frequency placement of reference signals on each antenna is used to avoid the interfering with each other. Thus, MIMO channel estimation may be addressed as the estimation of M × N individual channels, where M is the number of transmit antennas and N is the number of receive antennas. As a result, channel estimation in MIMO can be taken as a combination of different single-input, SISO estimations [14].

3.1.2 Pilot-based Channel Estimation Algorithms

When training symbols are used to estimate channel characteristics, the least-square (LS) and minimum-mean-square-error (MMSE) techniques are commonly used for channel estimation [15, 25-28, 30, 31].

The first assumption that is taken is all subcarriers are orthogonal, i.e. inter carrier interference (ICI) free. The representation of the diagonal matrix of training symbols for N subcarriers is as follows.

$$X=\begin{bmatrix} X[0] & 0 & - & 0 \\ 0 & X[1] & \cdots & 0 \\ \vdots & : & \ddots & \vdots \\ : & : & : & 0 \\ 0 & 0 & \cdots & X[N-1] \end{bmatrix} \quad \text{..... (3.4)}$$

Where X[k] denotes a pilot tone at the k^{th} subcarrier, with $E\{X[k]\} = 0$ *and* $Var\{X[k]\} = \sigma_x^2$, *k=0, 1, 2, ..., N-1*. By assumption that all the subcarriers are orthogonal, X is a diagonal matrix. Representing the channel gain by H[k] for each subcarrier k, the received training signal Y[k] can be represented as

$$Y \triangleq \begin{bmatrix} Y[0] \\ Y[1] \\ \vdots \\ \vdots \\ Y[N-1] \end{bmatrix} = \begin{bmatrix} X[0] & 0 & - & 0 \\ 0 & X[1] & \cdots & 0 \\ \vdots & : & \ddots & \vdots \\ : & : & : & 0 \\ 0 & 0 & \cdots & X[N-1] \end{bmatrix} \begin{bmatrix} H[0] \\ H[1] \\ \vdots \\ \vdots \\ H[N-1] \end{bmatrix} + \begin{bmatrix} Z[0] \\ Z[1] \\ \vdots \\ \vdots \\ Z[N-1] \end{bmatrix} \text{..... (3.5)}$$

$$Y=XH+Z$$

Where H is a channel vector given as $H=[H[0], H[1], \ldots, H[N-1]]^T$ and Z is a noise vector given as $Z=[Z[0], Z[1], \ldots, Z[N-1]]^T$ with $E\{Z[k]\}=o$ and $Var\{Z[k]\}= \sigma_z^2$, k=0,1,…, N-1.

3.1.2.1 Least Square Channel Estimation (LS) Technique

Denoting the channel estimate by $\hat{H}$ the Least Square Channel estimation technique gets the channel estimate by minimizing the following cost function [15]:

$$J(\hat{H}) = \left\| Y - X\hat{H} \right\|^2$$

$$= (Y - X\hat{H})^H (Y - X\hat{H}) \quad \text{.....(3.6)}$$

$$= Y^H Y - Y^H X\hat{H} - \hat{H}^H X^H Y + \hat{H}^H X^H X\hat{H}$$

In order to minimize we set the derivative of the function with respect to $\hat{H}$ zero, i.e.

$$\frac{\partial J(\hat{H})}{\partial \hat{H}} = -2(X^H Y)^* + 2(X^H X\hat{H})^* = 0 \quad \text{..... (3.7)}$$

Computing Equation 3.7 we get, $X^H X\hat{H} = X^H Y$ and from this we get the solution to the LS channel estimation as

$$\hat{H}_{LS} = X^H X^{-1}(X^H)^{-1}Y = X^{-1}Y \quad \text{..... (3.8)}$$

Denoting each component of the LS channel estimate $\hat{H}_{LS}$ by $\hat{H}_{LS}[k]$, where k=0, 1… N-1, based on the assumption of orthogonality i.e. ICI free mode, the Least square channel estimate $\hat{H}_{LS}$ can be written for each sub carrier as the following equation:

$$\hat{H}_{LS}[k] = \frac{Y[k]}{X[k]}, \quad \text{where } k=0,1,2,\ldots, N-1 \quad \text{.....(3.9)}$$

After having $\hat{H}_{LS}$ the LS channel estimate, we can calculate the Mean Square Error (MSE) of the LS channel estimation technique by

$$\begin{aligned} MSE_{LS} &= E\{(H - \hat{H}_{LS})^H (H - H_{LS})\} \\ &= E\{(H - X^{-1}Y)^H (H - X^{-1}Y)\} \\ &= E\{(X^{-1}Z)^H (X^{-1}Z)\} \\ &= E\{Z^H (XX^H)^{-1} Z\} \\ &= \frac{\sigma_z^2}{\sigma_x^2} \end{aligned} \quad \text{..... (3.10)}$$

As shown in Equation 3.10 the MSE of LS channel estimation is inversely proportional to Signal to Noise Ratio (SNR) $\frac{\sigma_x^2}{\sigma_z^2}$, it implies that it may be subject to noise enhancement, especially when the channel is in a deep null. Although LS technique has the above problem, as a result of mathematical simplicity it has been widely used for channel estimation [15].

3.1.2.2 Minimum Mean Square Channel Estimation Technique

Take the Least Square solution in the Equation 3.8 $\widehat{H}_{LS} = X^{-1}Y \triangleq \widetilde{H}$ and using a weight matrix W, define $\widehat{H} \triangleq W\widetilde{H}$ which corresponds to minimum mean square error estimate (MMSE) [15].

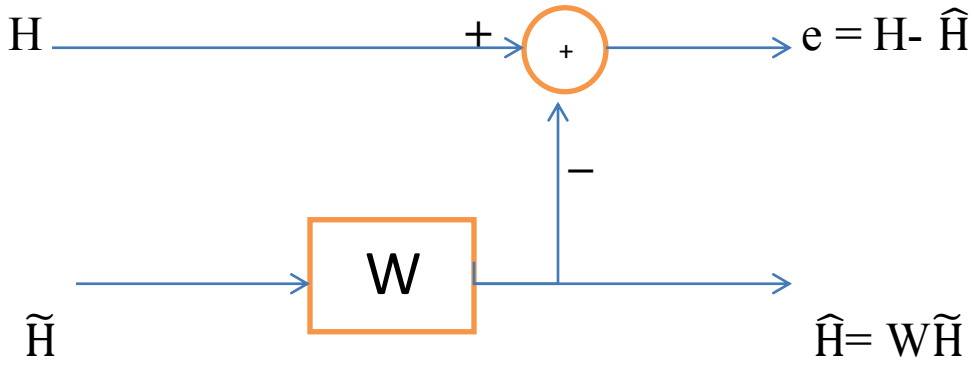

Figure 3.4 Minimum Mean Square Error channel Estimation [15].

From the Figure 3.4 we can see that MSE of the channel estimate $\widehat{H}$ is given by

$$J(\widehat{H}) = E\{\|e\|^2\} = E\{\|H - \widehat{H}\|^2\} \quad \text{..... (3.11)}$$

From this the MMSE channel estimation method finds a better estimate in terms of W in such a way that the MSE in Equation 3.10 is minimized. The orthogonality principle states that the estimation error vector $e = H - \widehat{H}$ is orthogonal to $\widetilde{H}$, such that

$$E\{e\widetilde{H}^H\} = E\{(H - \widehat{H})\widetilde{H}^H\}$$

$$= E\{(H - W\widetilde{H})\widetilde{H}^H\} \quad \text{..... (3.12)}$$

$$= E\{(H\tilde{H}^{H}\} - WE\{\tilde{H}\tilde{H}^{H}\}$$

$$= R_{H\tilde{H}} - WR_{\tilde{H}\tilde{H}} = 0$$

Where $R_{H\tilde{H}}$ is the cross correlation matrix of NxN matrices H and $\tilde{H}$ (i.e, $R_{H\tilde{H}} = E[H\tilde{H}^{H}]$), and $\tilde{H}$ is the Least Square channel estimate given by

$$\tilde{H} = X^{-1}Y = H + X^{-1}Z \qquad \text{.....(3.13)}$$

Solving Equation 3.12 for W results

$$W = R_{H\tilde{H}} R_{\tilde{H}\tilde{H}}^{-1} \qquad \text{.....(3.14)}$$

Where $R_{\tilde{H}\tilde{H}}$ is the auto correlation matrix of $\tilde{H}$ given by

$$R_{\tilde{H}\tilde{H}} = E\left\{\tilde{H}\tilde{H}^{H}\right\}$$

$$= E\{X^{-1}Y(X^{-1}Y)^{H}\}$$

$$= E\{(H + X^{-1}Z)(H + X^{-1}Z)^{H}\} \qquad \text{.....(3.15)}$$

$$= E\{HH^{H} + X^{-1}ZH^{H} + HZ^{H}(X^{-1})^{H} + X^{-1}ZZ^{H}(X^{-1})^{H}\}$$

$$= E\{HH^{H}\} + E\{X^{-1}ZZ^{H}(X^{-1})^{H}\}$$

$$= E\{HH^{H}\} + \frac{\sigma_z^2}{\sigma_x^2}I$$

And $R_{H\tilde{H}}$ is the cross-correlation matrix between the true channel vector and temporary channel estimate vector in the frequency domain. From the Equation 3.15, the MMSE channel estimate solved as:

$$\hat{H} = W\tilde{H}$$

$$= R_{H\tilde{H}} R_{\tilde{H}\tilde{H}}^{-1} \tilde{H}$$

$$= R_{H\tilde{H}} \left(R_{HH} + \frac{\sigma_z^2}{\sigma_x^2} I\right)^{-1} \tilde{H} \qquad \text{.....(3.16)}$$

The elements of $R_{H\tilde{H}}$ and R_{HH} in the above Equation 3.16 are

$$E\{h_{k,l} \tilde{h}^*_{k',l'}\} = E\{h_{k,l} h^*_{k',l'}\} = r_f[k-k'] r_t[l-l'] \qquad \text{.....(3.17)}$$

where k and l denote the subcarrier (frequency) index and OFDM symbol (time) index, respectively.

3.2 Blind Channel Estimation

The blind channel estimation is done by evaluating the statistical information of the channel and particular properties of the transmitted signals. The blind channel estimation has no overhead loss and it is only suitable for slowly time-varying channels. Blind channel estimation is used when the input of the channel is not available for processing at the receiver. Blind channel estimation techniques use the second-order statistics that contain sufficient information for the identification and estimation of finite impulse response channels [33, 34].

There are different suggested approaches in achieving the blind channel estimation and for further reading on blind channel estimation for MIMO-OFDM system [35-38].

3.3 Semi Blind Channel Estimation

Semi blind channel estimation techniques combine the approach of channel estimation both utilizing pilot sequences and a blind method to estimate the channel. Different approaches have been developed and suggested in the past few years [32, 39 and 40].

4. Mobile Radio Propagation Channel Characteristics

For appropriate designing and deployment of any wireless network, we need to have good understanding of the radio propagation environment. Radio propagation characteristics can vary depending on the terrain, frequency of operation, velocity of the mobile terminal, interference sources and other dynamic factors. Characterization of the radio channel using different parameters is useful for predicting signal coverage, achievable data rates, analysis of interference from different systems and determining the optimum location of base station antennas. Apart from line-of-sight communication, reflection, diffraction and scattering are the three fundamental factors that impact signal propagation in a mobile communication system [41]. For theoretical study, the environment is modeled as large-scale and small-scale models.

4.1 Large-scale Fading

Large-scale propagation models predict the mean signal strength for an arbitrary transmitter-receiver separation distance. Alternatively, the models characterize signal strength over large transmitter-receiver separation distance and they are useful in estimating the radio coverage area of a transmitter [16].

4.2 Small-scale fading

In the other case, modeling the propagation that characterize the rapid fluctuations of the received signal strength over very short travel distances (a few wavelengths) or short time durations (on the order of seconds) are called *small-scale* or fading models [16].

The Small scale fading, or, simply fading, means rapid fluctuations of the amplitudes, phases, or multipath delays of a radio signal over a short period or short travel distance. The large scale radio propagation loss effects might be ignored since the effect of small fading can be so severe.

Fading is caused by interference between two or more versions of the transmitted signal which arrive at the receiver at slightly different times. Depending on the distribution of the intensity and relative propagation time of the waves and the bandwidth of the transmitted signal, the multipath waves combined at the receiver antenna to give a resultant signal which can vary widely in amplitude and phase [16]. The knowledge and accurate understanding of the propagation channel fading in digital communication like LTE technology is very important since it improves the quality of communication.

4.3 Multipath Propagation and Small-scale fading

Multipath in wireless telecommunications is the propagation phenomenon that results in radio signals reaching the receiving antenna by two or more paths which impacts in propagation length variation and results in different time delays [47]. The effect of multipath includes constructive and destructive interference, and phase shifting of the signal. The three main effects of small scale multipath fading are:

a) Rapid fluctuation in signal strength over a small travel distance or time interval;
b) Random frequency modulation due to varying Doppler shifts on different multi path signal;
c) Time dispersion or echoes caused by multipath propagation delays.

From the many physical factors in the radio propagation channel that influence small scale fading are multipath propagation, the speed of the mobile(results in a Doppler shift), the speed of the surrounding objects(results in time varying Doppler shift) and the transmission bandwidth of the signal [16].

4.4 Mobile Multipath Channels Parameters

4.4.1 Time Dispersion Parameters

Power delay profile gives the intensity of a signal received through a multipath channel as a function of time delay. From power delay profile, we can determine the multipath channel parameters, the mean excess delay, root mean square (r.m.s) delay spread, and excess delay spread (X dB) [16]. The time dispersive properties of wide band multipath channels are usually quantified by their mean excess delay ($\bar{\tau}$) and r.m.s delay spread (σ_{τ}).

Mean excess delay is the first moment of the power delay profile and r.m.s delay spread is the square root of the second central moment of the power delay profile. For k number of taps;

Mean access delay

$$\bar{\tau}=\frac{\sum_k a_k^2 \tau_k}{\sum_k a_k^2}=\frac{\sum_k P(\tau_k)\tau_k}{\sum_k P(\tau_k)} \quad \text{.....[16] (4.1)}$$

And rms delay

$$\sigma_{\tau}=\sqrt{\overline{\tau^2}-(\bar{\tau})^2} \quad \text{.....[16] (4.2)}$$

Where τ_k is delay , $P(\tau_k)$ is attenuation of the k[th] multipath component and

$$\overline{\tau^2}=\frac{\sum_k a_k^2 \tau_k^2}{\sum_k a_k^2}=\frac{\sum_k P(\tau_k)\tau_k^2}{\sum_k P(\tau_k)}$$

4.4.2 Excess Delay and Coherence Bandwidth

Maximum Excess Delay (X dB) of the power delay profile is defined to be the time delay during which multipath energy falls to X dB below the maximum. Equivalently, the maximum excess delay is defined as τ_x-τ_0 , where τ_0 is the first arriving signal and τ_x is the maximum delay at which a multipath component is within X dB of the strongest arriving multipath signal [16].

Coherence bandwidth is used to characterize the channel in the frequency domain similar to the delay spread parameters in the time domain, Coherence bandwidth, B_C, is a statistical measure of the range of frequencies over which the channel can be considered "flat" meaning that a channel which passes all spectral components with approximately equal gain and linear phase. Equivalently, coherence bandwidth is the range of frequencies over which two frequency components have a strong potential for amplitude correlation [16].

4.4.3 Doppler Spread and Coherence Time

The time varying nature of the channel caused by either relative motion between the mobile and base station, or by movement of objects in the channel is not described by the time dispersive parameters, delay spread and coherence bandwidth. Doppler spread and coherence time are the parameters to describe the time varying nature of the channel. Doppler spread B_D is a measure of the spectral broadening caused by the time rate of change of the mobile radio channel and is defined as the range of frequencies over which the received Doppler spectrum is essentially non-zero. Coherence time T_C is the time domain dual of Doppler spread and is used to characterize the time varying nature of the frequency dispersive-ness of the channel in the time domain. The Doppler spread and coherence time are inversely proportional to one another [16]. That is,

$$T_C = \frac{1}{f_m} \qquad \text{..... (4.3)}$$

4.5 Small Scale Fading Types

Based on the relation between the signal parameters (bandwidth, symbol period) and the channel parameters (r.m.s delay spread and Doppler spread), we have four different cases of fading. Due to time dispersive nature we have Flat and Frequency selective fading and due to Doppler spread we have fast and slow fading [16].

4.5.1 Fading Effects due to Multipath Time Delay Spread

4.5.1.1 Flat Fading

When the bandwidth of the transmitted signal is less than the coherence bandwidth of the channel we call it Flat Fading. Expressing with the different term, Flat fading occurs when the symbol period of the signal is more than the r.m.s delay spread of the channel [16].
Flat fading occurs when

$$B_S << B_C \text{ and } T_S >> \sigma_T \quad \text{---------- (4.4)}$$

Where B_S is the signal bandwidth and B_C is the coherence bandwidth, T_S is the symbol period and σ_T is the r.m.s delay spread. At Flat fading the mobile channel has a constant gain and linear phase response over its bandwidth.

4.5.1.2 Frequency Selective Fading

When the signal bandwidth is more than the coherence bandwidth of the mobile radio channel or equivalently the symbols duration of the signal is less than the rms delay spread [16], frequency selective fading occurs.

$$\text{i.e., } B_S >> B_C \text{ and } T_S << \sigma_T \quad \text{---------- (4.5)}$$

At the receiver, we obtain multiple copies of the transmitted signal, all attenuated and delayed in time. The channel introduces inter symbol interference [16]. A rule of thumb which is dependent on the type of modulation used for a channel to have flat fading is if

$$\sigma_T / T_s \leq 0.1 \quad \text{---------- (4.6)}$$

4.5.2 Fading Effects due to Doppler Spread

4.5.2.1 Fast Fading

When the channel impulse response changes rapidly within the symbol duration of the signal fast fading occurs. Since coherence time of the channel is smaller than the symbol period of the transmitted signal it results in Doppler spreading, as a result a signal undergoes frequency dispersion leading to distortion [16]. A signal undergoes fast fading if

$$T_S >> T_C \text{ and } B_S >> B_D \quad \text{---------- (4.7)}$$

Where T_C is the coherence time and B_D is the Doppler spread.

4.5.2.2 Slow Fading

In such a channel, rate of the change of the channel impulse response is much less than the transmitted signal. We can consider a slow faded channel as a channel in which the channel is almost constant over at least one symbol duration [16]. Thus slow fading occurs when

$$T_S << T_C \text{ and } B_S >> B_D \quad \text{---------- (4.8)}$$

We can observe that the velocity of the user has an important factor in deciding whether the signal experiences fast or slow fading.

4.6 ITU Multipath Fading Propagation Conditions for LTE

According to [43, 44] the multipath propagation conditions are made of firstly a delay profile in the form of a "tapped delay-line", characterized by a number of taps at fixed positions on a sampling grid. And further the profile can be characterized by the r.m.s. delay spread and the

maximum delay spanned by the taps. Secondly, a combination of channel models parameters that consist of the delay profile and the Doppler spectrum that is characterized by a classical spectrum shape and a maximum Doppler frequency. Finally it is made of a set of correlation matrices defining the correlation between the UE and eNodeB antennas in the case of multi-antenna systems. In addition, additional multi-path models used for Channel Quality Indication tests can be included.

There exists an important difference between the methods of specifying propagation conditions for LTE and for UMTS. The delay profiles are specified for different UE velocities in UMTS. Thus for performance testing, each frequency band requires a different set of Doppler frequencies. In LTE, it was decided to fix the Doppler frequencies for the EPA, EVA, ETU, and high speed train profiles and apply these to all frequency bands in order to reduce the test burden. As a result the effective UE velocity has now become variable as a function of the test frequency, and for the high speed train case, the inter-site distances have also become variable. This approach is not as pure as the fixed velocity approach for UMTS; nevertheless, fixing the Doppler frequencies is expected to provide sufficient test coverage with the benefit of significant test simplification.

4.6.1 Delay Profiles

ITU recommend delay profiles for LTE UE receiver testing that are selected to represent low, medium and high delay spread environments. The three delay profiles defined are: one for pedestrian use, one for vehicular use, and one for typical urban use as shown in Table 4.1. These delay profiles are used in this thesis work for simulation.

Model	**Number of channel taps**	**Delay spread (r.m.s.)**	**Maximum excess tap delay (span)**
Extended Pedestrian A model (EPA)	7	45 ns	410 ns
Extended Vehicular A model (EVA)	9	357 ns	2510 ns
Extended Typical Urban model (ETU)	9	991 ns	5000 ns

Table 4.1 Delay profiles for E-UTRA channel models [36.101 [43] Table B.2.1-1].

Propagation conditions are specified in 36.101[43] Annex B. A delay profile for a typical pedestrian, Vehicular and Typical Urban environment is given in following tables Table 4.2, Table 4.3 and Table 4.4 respectively.

Excess tap delay [ns]	Relative power [dB]
0	0.0
30	-1.0
70	-2.0
90	-3.0
110	-8.0
190	-17.2
410	-20.8

Table 4.2 Extended Pedestrian A model (EPA) [36.101 [43] Table B.2.1-2].

Excess tap delay[ns]	Relative power [dB]
0	0.0
30	-1.5
150	-1.4
310	-3.6
370	-0.6
710	-9.1
1090	-7.0
1730	-12.0
2510	-16.9

Table 4.3 Extended Vehicular A model (EVA) [36.101 [43] Table B.2.1-3]

Excess tap delay [ns]	Relative power [dB]
0	-1.0
50	-1.0
120	-1.0
200	0.0
230	0.0
500	0.0
1600	-3.0
2300	-5.0
5000	-7.0

Table 4.4 Extended Typical Urban model (ETU) [36.101 [43] Table B.2.1-4].

4.6.2 Combinations of Channel Model Parameters

Specifying the maximum Doppler frequency shift in addition to the delay profile is very important. The three different frequencies that are used to represent low, medium, and high speeds are 5 Hz, 70 Hz, and 300 Hz, respectively. For 2GHz

1) 5 Hz Doppler for which the relative UE velocity has been defined to be 2.7 km/h;
2) 70 Hz Doppler for which the relative UE velocity has been taken to be 37.8 km/h;
3) 300 Hz Doppler for which the relative UE velocity has been calculated to be 162 km/h.

The maximum Doppler frequencies are combined with the delay profiles to produce the combinations that are used to define the receiver performance requirements. From possible combination of three delay profiles and three Doppler frequencies, only five of them combinations are used [44]. Table 4.5 shows propagation conditions that are used for the performance measurements in multi-path fading environment for low, medium and high Doppler frequencies.

Model	Maximum Doppler frequency
EPA 5Hz	5 Hz
EVA 5Hz	5 Hz
EVA 70Hz	70 Hz
ETU 30Hz	30 Hz
ETU 70Hz	70 Hz
ETU 300Hz	300 Hz

Table 4.5 Channel model parameters [36.101 [43] Table B.2.2-1].

In [44] it is described that the pedestrian profile is defined for the low speed 5 Hz Doppler frequency only; the vehicular profile is defined for 5 Hz and 70 Hz only; and the typical urban profile excludes the 5 Hz case. The additional delay profile that has been defined is specifically for high speed trains.

4.6.3 MIMO Fading Channel Characteristics

For an antenna configuration using uniform linear arrays at both eNodeB and UE, the MIMO channel correlation matrices are defined in [43]. The eNodeB and UE correlation matrix are described in Table 4.6.

	One antenna	Two antennas	Four antennas
eNodeB Correlation	$R_{eNB}=1$	$R_{eNB}=\begin{pmatrix} 1 & \alpha \\ \alpha^* & 1 \end{pmatrix}$	$R_{eNB}=\begin{pmatrix} 1 & \alpha^{1/} & \alpha^{/} & \alpha \\ \alpha^{1/*} & 1 & \alpha^{1/} & \alpha^{/} \\ \alpha^{/*} & \alpha^{1/*} & 1 & \alpha^{1/} \\ \alpha^{*} & \alpha^{/*} & \alpha^{1/*} & 1 \end{pmatrix}$
UE Correlation	$R_{UE}=1$	$R_{eNB}=\begin{pmatrix} 1 & \beta \\ \beta^* & 1 \end{pmatrix}$	$R_{UE}=\begin{pmatrix} 1 & \beta^{1/} & \beta^{/} & \beta \\ \beta^{1/*} & 1 & \beta^{1/} & \beta^{/} \\ \beta^{/*} & \beta^{1/*} & 1 & \alpha^{1/} \\ \beta^{*} & \beta^{/*} & \beta^{1/*} & 1 \end{pmatrix}$

Table 4.6 eNodeB and UE correlation matrix [36.101 [43] Table B.2.3.1-1, Table B.2.3.1.2].

The channel spatial correlation matrix R_{spat} is defined in Table 4.7. The parameters α and β in Table 4.6 and Table 4.7 defines the spatial correlation between the antennas at the eNodeB and UE.

1x2 case	$R_{spat}=R_{UE}=\begin{bmatrix} 1 & \beta \\ \beta^* & 1 \end{bmatrix}$
2x2 case	$R_{spat}=R_{eNB}\otimes R_{UE}=\begin{bmatrix} 1 & \alpha \\ \alpha^* & 1 \end{bmatrix}\otimes\begin{bmatrix} 1 & \beta \\ \beta^* & 1 \end{bmatrix}=\begin{bmatrix} 1 & \beta & \alpha & \alpha\beta \\ \beta^* & 1 & \alpha\beta^* & \alpha \\ \alpha^* & \alpha^*\beta & 1 & \beta \\ \alpha^*\beta^* & \alpha^* & \beta^* & 1 \end{bmatrix}$

4x2 case	$R_{spat} = R_{eNB} \otimes R_{UE} = \begin{bmatrix} 1 & \alpha^{1/9} & \alpha^{4/9} & \alpha \\ \alpha^{1/9*} & 1 & \alpha^{1/9} & \alpha^{4/9} \\ \alpha^{4/9*} & \alpha^{1/9*} & 1 & \alpha^{1/9} \\ \alpha^{*} & \alpha^{4/9*} & \alpha^{1/9*} & 1 \end{bmatrix} \otimes \begin{bmatrix} 1 & \beta \\ \beta^{*} & 1 \end{bmatrix}$
4x4 case	$R_{spat} = R_{eNB} \otimes R_{UE} = \begin{bmatrix} 1 & \alpha^{1/9} & \alpha^{4/9} & \alpha \\ \alpha^{1/9*} & 1 & \alpha^{1/9} & \alpha^{4/9} \\ \alpha^{4/9*} & \alpha^{1/9*} & 1 & \alpha^{1/9} \\ \alpha^{*} & \alpha^{4/9*} & \alpha^{1/9*} & 1 \end{bmatrix} \otimes \begin{pmatrix} 1 & \beta^{1/9} & \beta^{4/9} & \beta \\ \beta^{1/9*} & 1 & \beta^{1/9} & \beta^{4/9} \\ \beta^{4/9*} & \beta^{1/9*} & 1 & \beta^{1/9} \\ \beta^{*} & \beta^{4/9*} & \beta^{1/9*} & 1 \end{pmatrix}$

Table 4.7 R_{spat} correlation matrices [[43] Table B.2.3.1-3]

For cases with more antennas at either eNodeB or UE or both, the channel spatial correlation matrix can still be expressed as the Kronecker product of R_{eNB} and R_{UE} according to $R_{spat} = R_{eNB} \otimes R_{UE}$.

The α and β for different correlation types are given in Table 4.8. These values are used for this thesis simulation.

Low correlation		**Medium Correlation**		**High Correlation**	
α	β	α	β	α	β
0	0	0.3	0.9	0.9	0.9

Table 4.8 MIMO Correlation Matrices at High, Medium and Low Level [36.101[43] Table B.2.3.2-1].

5. Analysis and Simulation

5.1 Simulation Model and Parameters

In order to achieve the goal of this thesis, the system model shown in Figure 5.1 of LTE MIMO-OFDM which uses transmit diversity mode of system (using SFBC coding and decoding) is used and the pilot based channel estimation methods are selected and performance of the LS and LMMSE channel estimation techniques are analyzed.

In this thesis as LTE transmit diversity mode is used in the simulation part, the MIMO 2x2 OFDM model is presented in the following block diagram Figure 5.1.

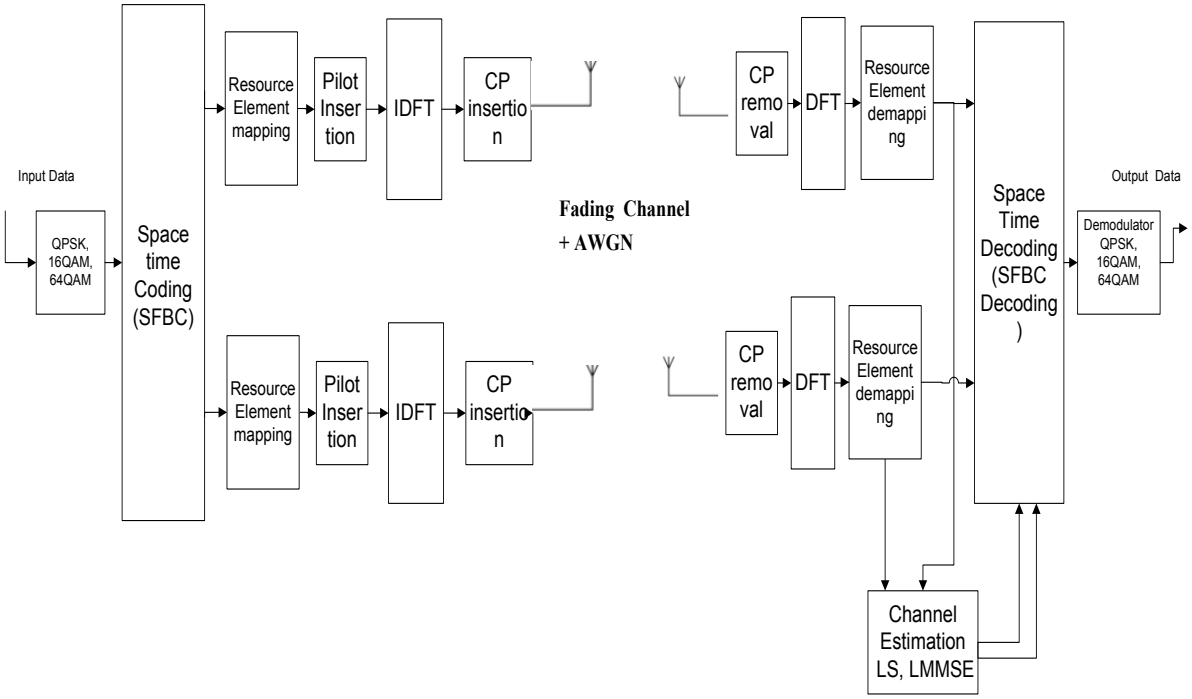

Figure 5.1 LTE 2X2 MIMO OFDM system.

And the general LTE physical layer specifications Physical Downlink Shared Channel (PDSCH) processing at the transmitter side which is used in the thesis simulation is illustrated in Figure 5.2.

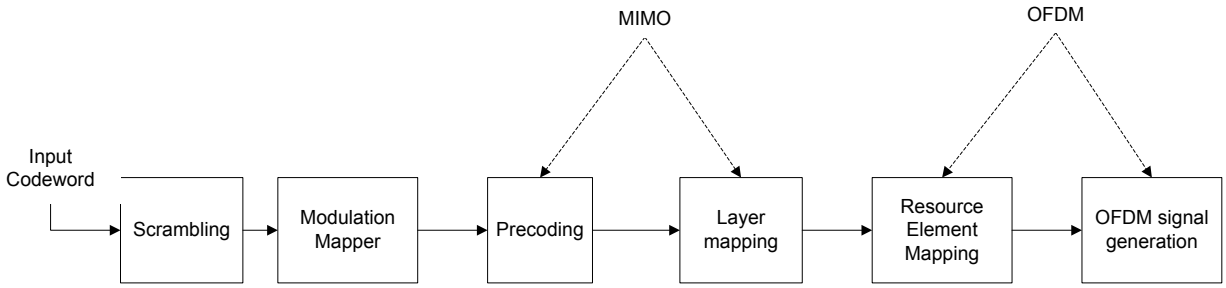

Figure 5.2 Down Link PDSCH processing of physical layer specifications in LTE.

As in Figure 5.2 the downlink physical channel processing includes:

Scrambling

The source data bits (transport channel encoded bits) are scrambled by a bit-level scrambling sequence. To ensure interference randomization between cells, the scrambling sequence depends on the physical layer cell identity. The thesis simulation assumes a single-user single-cell downlink transmission and takes a 0 cell ID.

Data Modulation

The scrambled bits are converted to complex modulated symbols in downlink data modulation. QPSK, 16QAM and 64QAM are the set of modulation schemes supported, corresponding to two, four, and six bits per modulation symbol.

Layer Mapping and Pre-coding

The space-frequency block coding specified for LTE is used in the simulation. For two schemes, the LTE specifications make use of the basic Alamouti code [22], applied over space and frequency dimensions.

Resource Element Mapping

The pre-coded symbols to be transmitted on each antenna are mapped to the resource elements of the resource blocks available for transmission. The number of available resource blocks is a function of the channel bandwidth parameter as in Table 2.3. Here in this thesis the simulation configuration 10MHz channel bandwidth with 50 available resource blocks is used. The actual number of data symbols mapped to resource elements per subframe depends on the resource elements occupied by CSR signals used for channel estimation and physical downlink control channel (PDCCH) resource elements occupied by primary synchronization signals (PSS) and secondary synchronization signals (SSS) resource elements occupied by transmission of the physical broadcast channel (PBCH).

OFDM Transmission

The complex-valued time-domain OFDM signal per antenna is generated from the fully populated resource grid. The number of FFT points depends on the channel bandwidth specified and normal cyclic prefix is used in the simulation.

MIMO Channel

The simulator uses a model of Rayleigh fading over multiple links. As per ITU test recommendations, EPA, EVA and ETU channel models are used with their Doppler shift, path gains, path delays and correlation levels for each link.

Receiver (UE) Processing

At the UE the elements in the receiver processing modeled in the simulation are the following. OFDM receiver converts back to the time- and frequency-domain grid structure. Channel estimation employs LMMSE and LS estimations and it uses averaging over a subframe for noise reduction for the reference signals, and linear interpolation over the subcarriers for the data elements for LS. This uses the CSR signals for the channel estimates. Transmit Diversity Combining for the multiple transmitted signals are used, similar to the encoder, which uses complex notation for signals. The combined data stream is further demodulated and descrambled to get the received data bits.

The simulations have been performed using MATLAB codes and below are parameters used in the simulation:

- Normal cyclic prefix is used;
- Number of frames sent for test is flexible using a loop in the code and for this particular simulation it is 10 frames;
- Flexible bandwidth of 1.4, 3, 5, 10, 15, 20 MHz, for this particular case 10MHz is used in the simulation;
- Cell ID number 0 configurations for pilot signal generation is used.

	Simulation parameter	**Values used**
1	Antenna type	2x2, 2x1
2	MIMO transmission mode	Transmit diversity
3	Number of subframes	50
4	Channel bandwidth	10MHz, 50 Resource Block
5	Modulation type	QPSK, 16QAM,64QAM
6	Cyclic prefix	Normal
7	MIMO correlation level	Low, Medium, High
8	Doppler Frequency	5Hz,70Hz, 120Hz, 300Hz
9	Cell ID number	0
10	Channel model	EPA, EVA, ETU
11	Channel estimation techniques	LS, LMMSE
12	Interpolation method	Linear

Table 5.1 Simulation parameters.

5.2 Simulation Results

The results drawn from the simulation at higher SNR are not smooth curves at some figures and this arise from limitation in the number of iteration, which results from limitation in computational capability of the computer used during the simulation. Bit Error Rate (BER) performance of LS and MMSE channel estimations for QPSK, 16QAM and 64QAM modulation schemes at low correlation level of 2x2 MIMO antennas for EPA channel model with 5Hz Doppler frequency is shown in Figure 5.3.

From Figure 5.3 we can see that the overall performance of LMMSE estimation method is better than LS estimation technique for QPSK and 16QAM modulation scheme at EPA channel model. As we move from lower modulation to higher modulation, in this case from QPSK to 16QAM, we can see that the BER performances of both estimation techniques (LS and LMMSE) BER performance are decreasing. But the performance gap between the two algorithms is different as we move from lower SNR to higher SNR at different modulation scheme.

For SNR less than 5dB (lower SNR region) we can see that LS and LMMSE estimation techniques with linear interpolation at QPSK, 16QAM and 64QAM is comparable and only the performance gap increases as SNR increases. In using QPSK as a lower modulation at EPA test channel model, the performance of the two algorithms started saturating for certain performance level at 20dB and the performance gap is comparable after 20dB. But in case of using 16QAM and 64QAM modulation order, LMMSE has a higher gain than LS; however, the relative gain diminishes at higher SNR regions, specifically for SNR >30 dB.

From the result in using 16QAM modulation scheme, we can see that for LMMSE, after 20dB the increase in performance as we increase SNR is diminishing and it will be a waste to increase SNR. The same is true for LS for SNR greater than 30dB.

The other point that needs to be mentioned from the simulation result is that the BER performance gap between LS and LMMSE as we go from lower modulation to higher

modulation is kept for low SNR and the gap is increasing as we move to higher SNR. For QPSK the performance has a clear wider gap between the two algorithms between 10dB to 20dB SNR regions, but for 16QAM the gap is wider between 15dB to 30dB SNR regions.

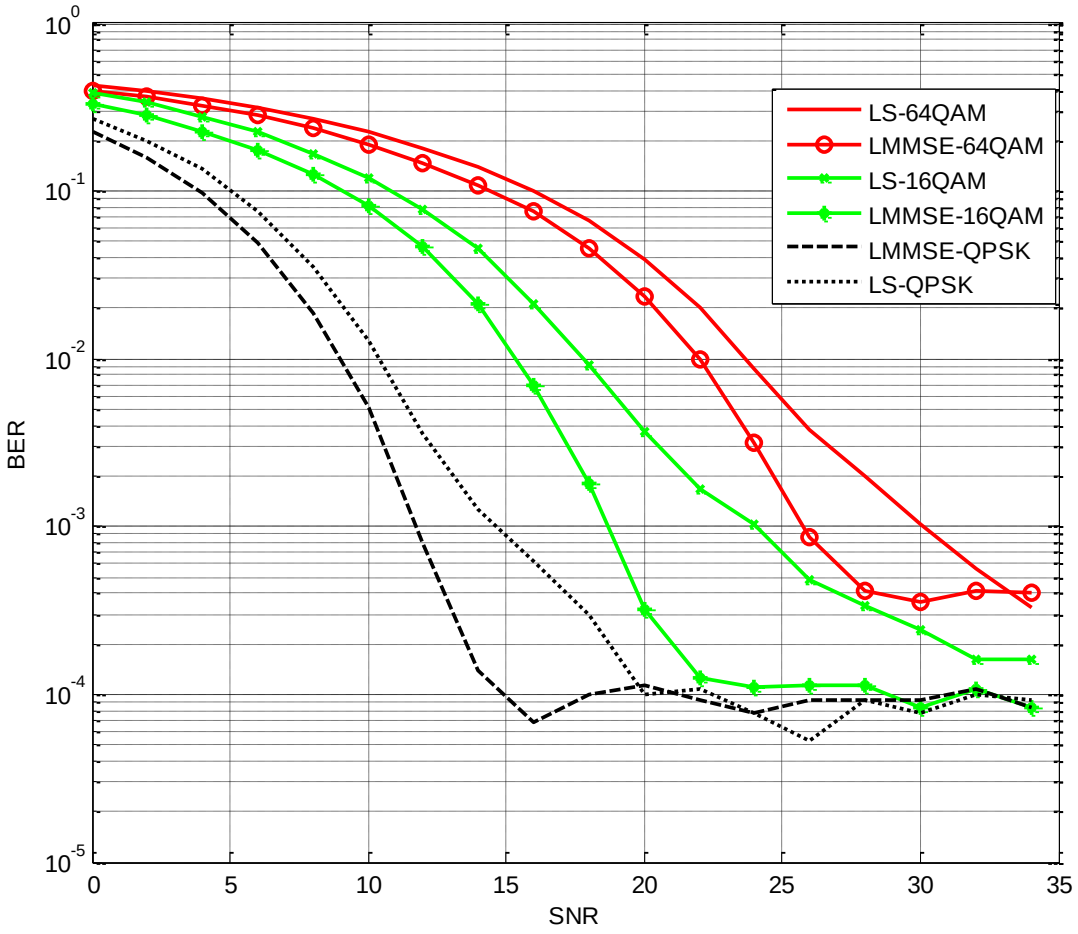

Figure 5.3 2x2 MIMO antenna with low correlation and using EPA channel model.

And BER performance of the two channel estimation techniques for LTE EVA and ETU channel model with 70Hz Doppler frequency for MIMO 2x2 antenna and QPSK and 16QAM modulation scheme results are shown in Figure 5.4 and Figure 5.5.

As can clearly be seen from Figure 5.4 and Figure 5.5 in general performance of LMMSE is superior to LS in both QPSK and 16QAM modulation schemes. We can, thus, generalize that at both EVA and ETU channel models performance of LMMSE is better than LS. In general it is

seen that for both channel models at SNR more than 25dB, the two algorithms started to be comparable. As the complexity of the operation for LS is simple over LMMSE, the use of LS for higher SNR is advisable.

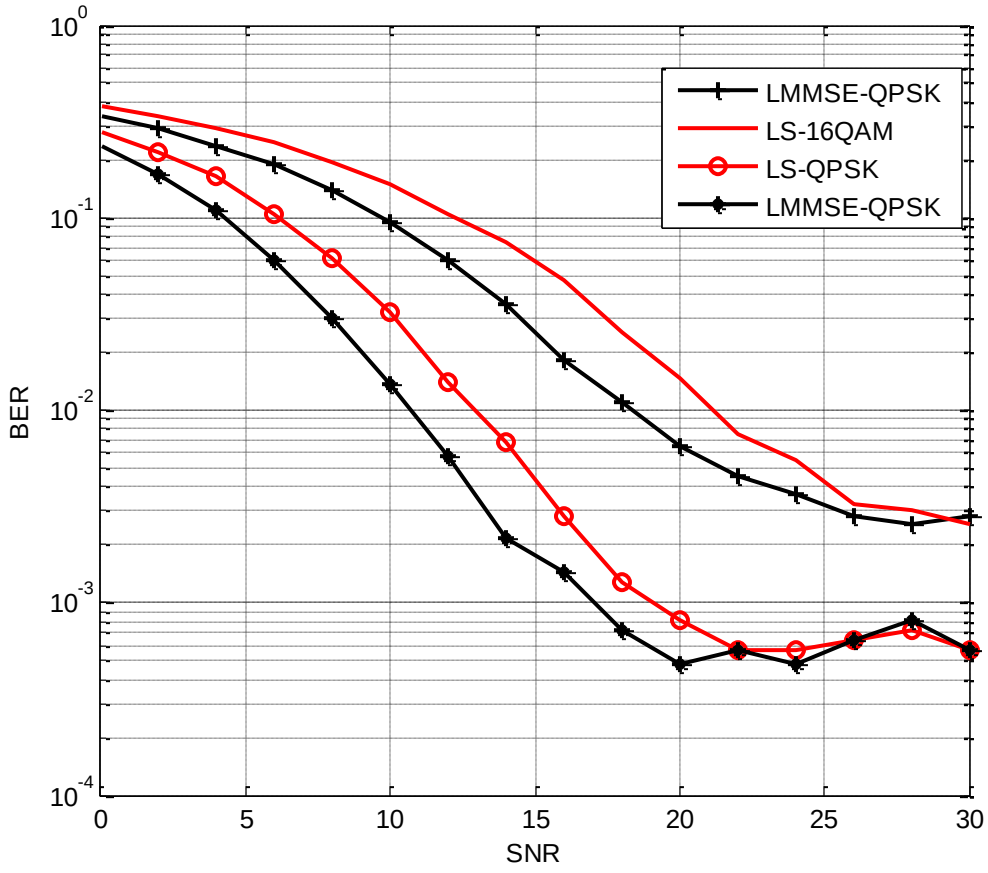

Figure 5.4 BER performance of LS and LMMSE for QPSK and 16QAM modulation using LTE EVA 70Hz channel model for 2x2 MIMO.

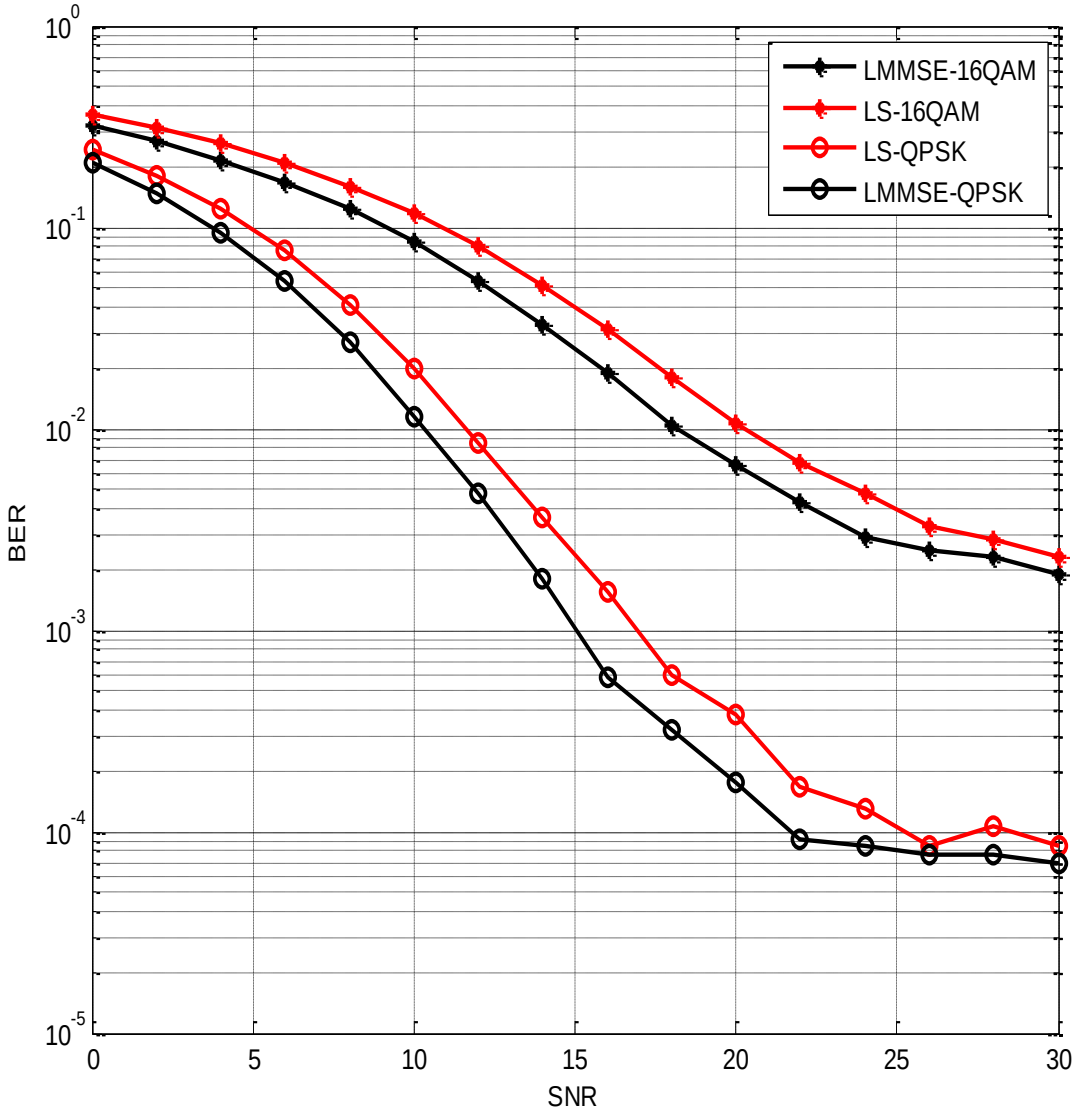

Figure 5.5 BER performance of LMMSE and LS channel estimation techniques for ETU-70Hz channel model.

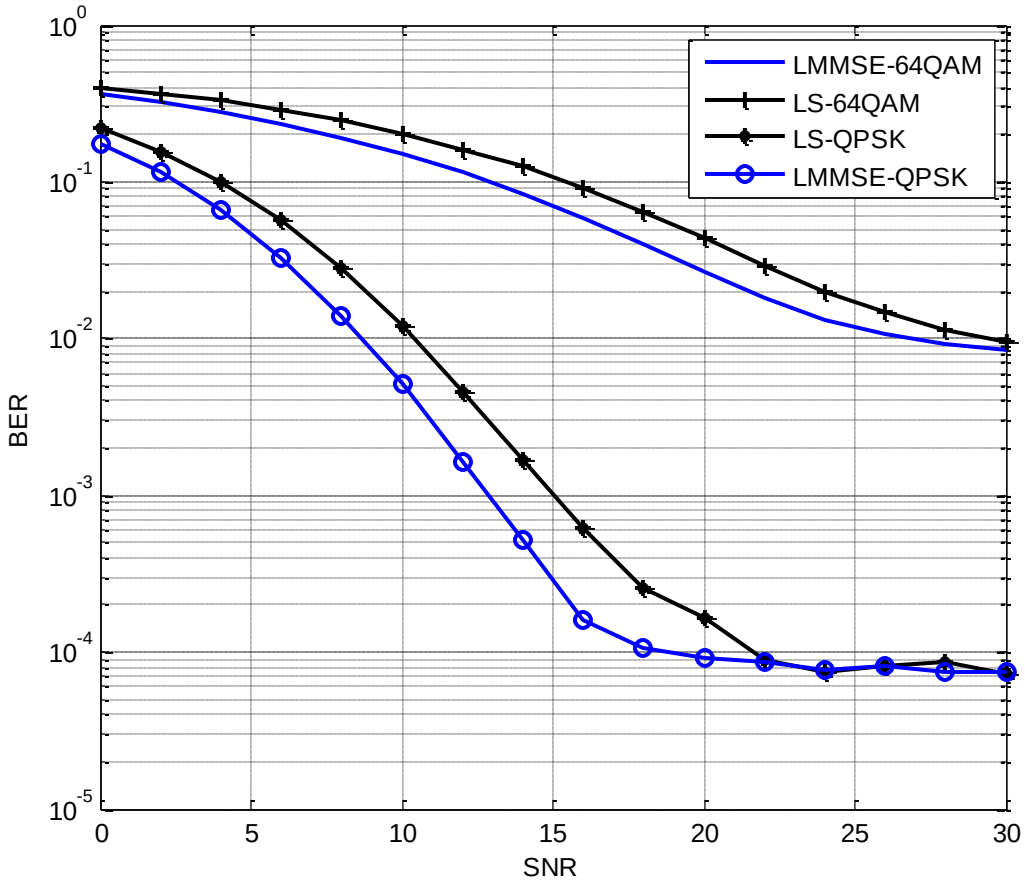

Figure 5.6 BER performance of LS and LMMSE for QPSK and 64QAM using EVA 70Hz channel model for 2x2 MIMO.

The BER performance of LS and LMMSE channel estimation technique for low correlation 2x2MIMO antenna and QPSK and 64QAM modulation at EVA 70HZ channel model is shown in Figure 5.6 above.

From Figure 5.6 it is seen that performance of LMMSE is superior for QPSK and 64QAM modulation than LS in using EVA channel model. But the performance gap is diminishing as we increase SNR and become comparable for higher SNR regions. The range of decease in gap varies for the two modulation schemes. For 64QAM the two algorithms become comparison for SNR>30dB and for QPSK it is for SNR> 22dB.

With low antenna correlation BER performance of LMMSE channel estimation technique for 2x1 and 2x2 MIMO antennas using 16QAM modulation scheme and EPA channel model with 5Hz Doppler frequency is shown in Figure 5.7.

From Figure 5.7 it is confirmed that the performance of LMMSE estimation for using 2x2 is superior to 2x1 because of the diversity gain of using multiple antennas at the receiver side.

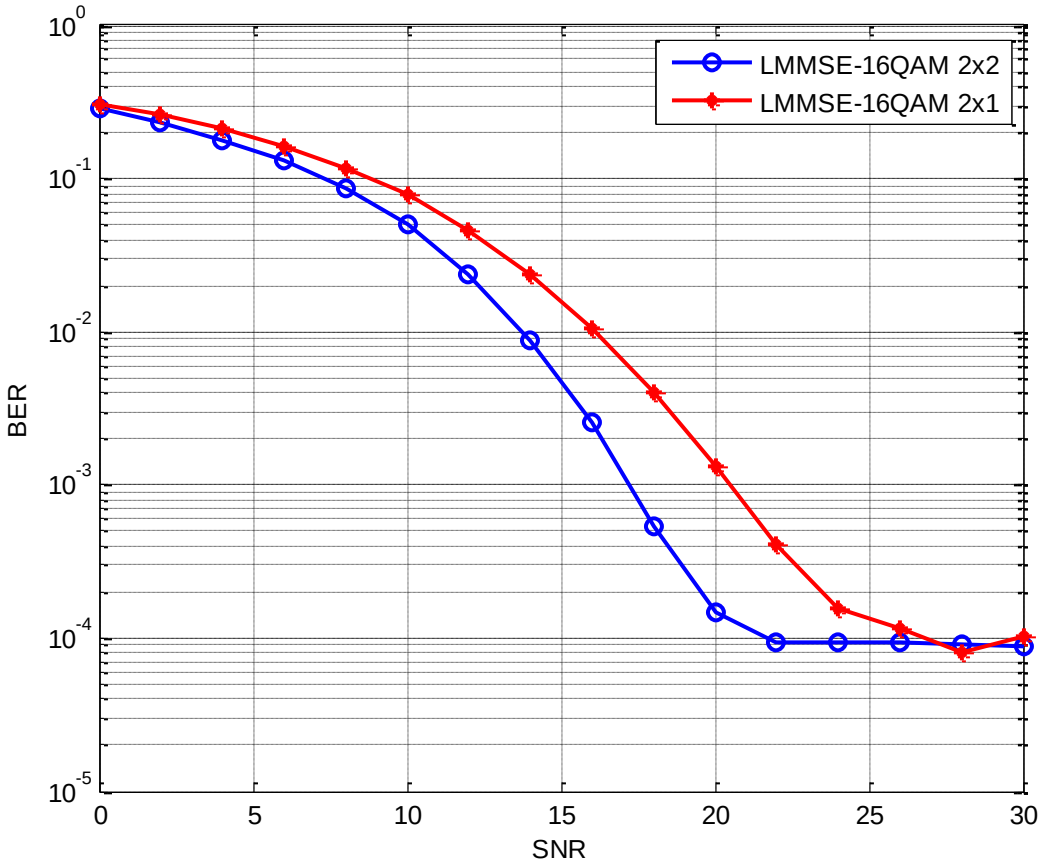

Figure 5.7 BER performance of LMMSE estimation for using 2x2 and 2x1 MIMO antennas.

The BER performance LMMSE channel estimation of using high (α=0.9 and β=0.9), medium (α=0.3 and β=0.9) and low correlation (α=0 and β=0) at EVA 5Hz channel model and with 16QAM modulation scheme is depicted at Figure 5.8.

As it is clearly seen in Figure 5.8 the use of low correlation antennas has the advantage on BER performance of the system over using high correlation antennas.

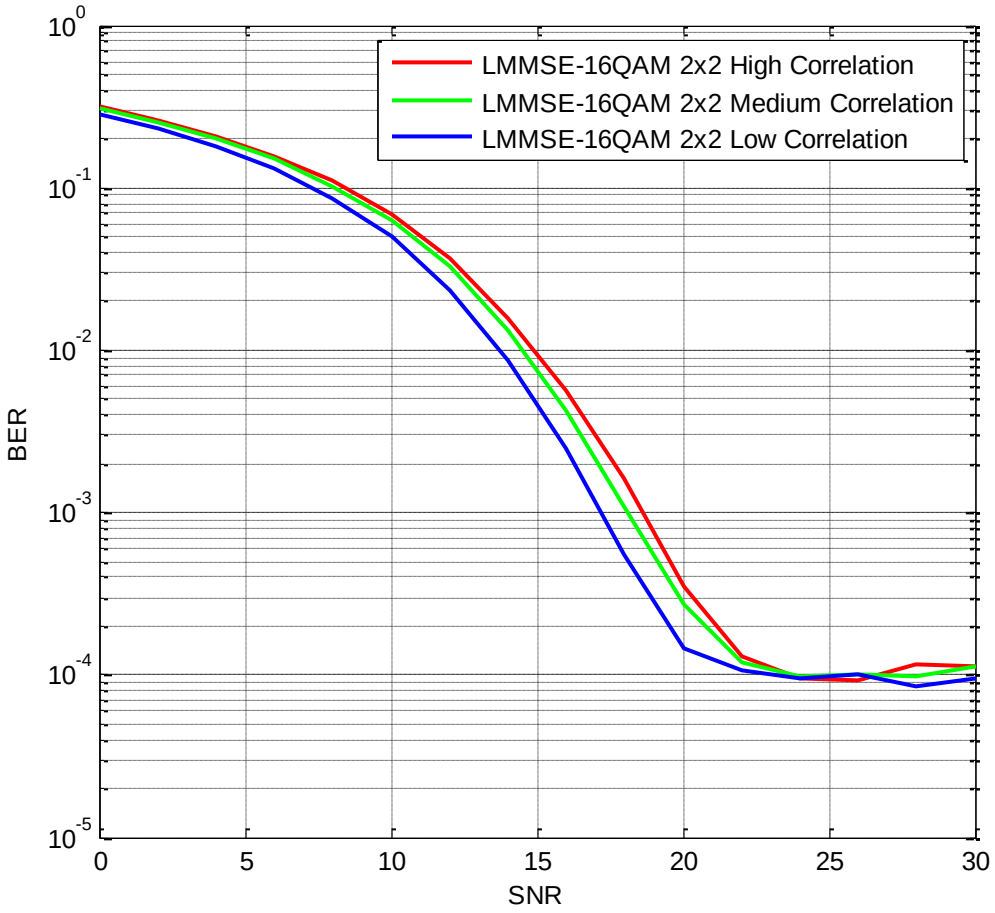

Figure 5.8 High Medium and Low correlation Level 2x2 MIMO for EPA 5Hz channel model.

The BER performance of the three ITU channel models i.e. EPA, EVA and ETU channel models for 2x2 MIMO using LMMSE channel estimation algorithms for 16QAM modulation scheme are depicted in the Figure 5.9 below.

In Figure 5.9 it is clearly seen that when there is an increase in Doppler frequency and an increase in delay spread in EVA and ETU channel models, the BER performance of LMMSE channel estimation is decline to be worst. It is clearly seen that speed of the mobile user and delay spread are determining factors on performance of the channel estimation.

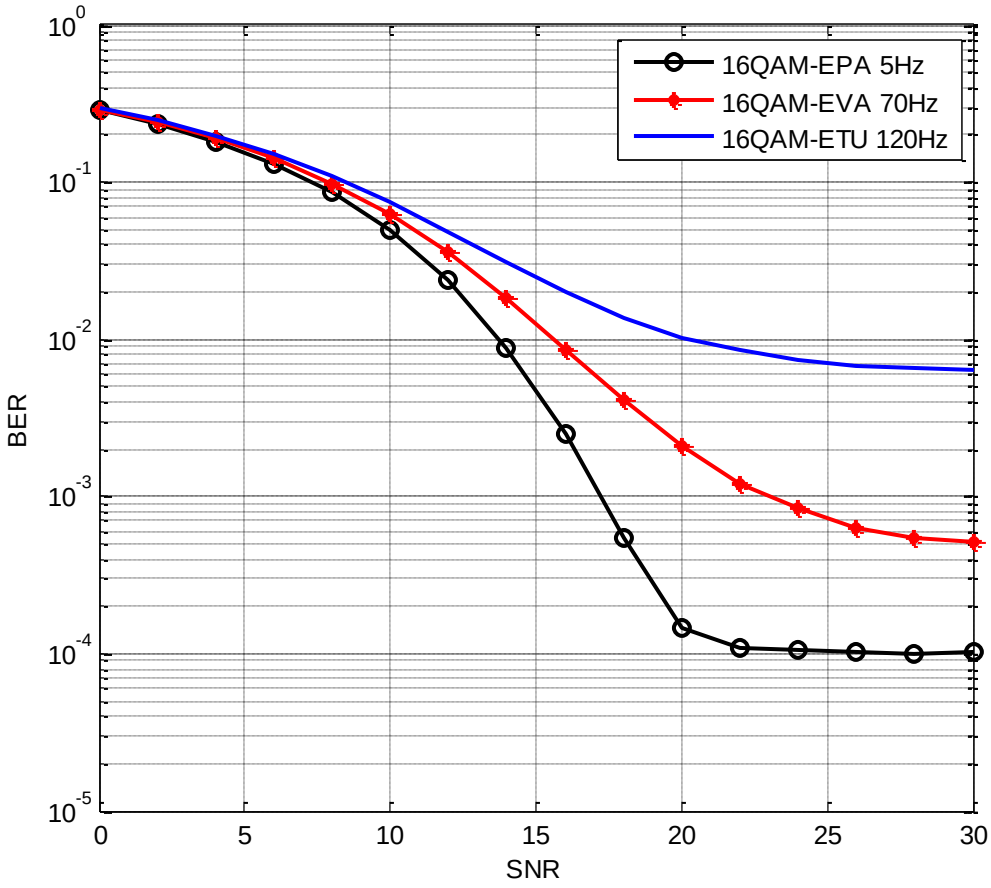

Figure 5.9 LMMSE performances for ETU, EVA and EPA channel models for 2x2 MIMO.

6. Conclusions and Recommendation for Future Work

The objective of the thesis was to evaluate the performance of channel estimation algorithms for LTE MIMO-OFDM downlink system in using higher modulation schemes. LS and LMMSE channel estimation techniques were selected and transmit diversity of the MIMO mode was used. MATLAB simulation method is used to analyze and present the results.

In this thesis pilot based channel estimation techniques is studied for LTE system using higher order modulations. For higher order modulation and at different ITU channel models such as EPA, EVA and ETU in general, LMMSE has a higher gain than LS; however, the relative gain diminishes at higher SNR regions, specifically for SNR >30 dB and the use of LS estimation technique due to its simplicity of operation is advisable. Similar results were reported in previous researches [10] for the same system and channel model types but for lower order modulations. In addition in the thesis, it is confirmed that the use of MIMO antenna has a good BER performance advantage over using single antenna in the receiver side.

The method that is used in the simulation is transmitting diversity mode of MIMO and Linear interpolation technique. The use of other interpolation methods can improve and be a future study for performance of the two channel estimation techniques. Furthermore study on performance of the two channel estimation techniques when spatial diversity mode of MIMO is used can be a window for future work. In addition, the use and implementation methods of blind and semi-blind channel estimation in LTE system is one of the emerging research areas that need to be investigated and can be a window for future work.

7. References

[1] Magdalena Nohrborg. *"LTE Overview"* Internet:www.3gpp.org/LTE [Dec. 1, 2014]

[2] Sweta M. Patil and Prof.A.N Jadhav. *"Channel Estimation Using LS and MMSE Estimators"* International Journal on Recent and Innovation Trends in Computing and Communication ISSN: 2321-8169 Volume: 2 Issue: 3

[3] R.S.Ganesh, Dr. J.Jaya Kumar. *"A Survey on Channel Estimation Techniques in MIMO-OFDM Mobile Communication Systems"* International Journal of Scientific & Engineering Research, Volume 4, Issue 5, May-2013

[4] Erik Dahlman, Stefan Parkvall and Johan Scöld. *4G:LTE/LTE-Advanced for Mobile Broadband,* 2nd Edition, Waltham, MA 02451, USA: Elsevier Ltd, 2014.

[5] Hala M. Abd Elkader, Gamal Mabrouk, Adly T. Eldien and Reham S. Saad, *"Performance of LTE Channel Estimation Algorithms for Different Interpolation Methods and Modulation Schemes"* International Journal of Engineering Research and Development, Volume 10, Issue 4 (April 2014), PP.48-52

[6] K.Rajeswari, T. Sangeetha, A.P Natchammai, M.Nandhini, and S. J. Thiruvengadam, *"Performance Analysis of Pilot Aided Channel Estimation Methods for LTE System in Time-Selective Channels"* 2010 5th International Conference on Industrial and Information Systems, ICIIS 2010, India ,Jul 29 - Aug 01, 2010

[7] Abdelhakim Khlifi and Ridha Bouallegue. *"Performance Analysis of LS and LMMSE Channel Estimation Techniques for LTE Downlink Systems*" International Journal of Wireless & Mobile Networks (IJWMN) Vol. 3, No. 5, October 2011

[8] Sinem Coleri, Mustafa Ergen, Anuj Puri, and Ahmad Bahai. *"Channel Estimation Techniques Based on Pilot Arrangement in OFDM Systems"* IEEE TRANSACTIONS ON BROADCASTING, Vol. 48, No. 3, September 2002

[9] Abdelhakim Khlifi and Ridha Bouallegu., *"Comparison between Performances of Channel estimation Techniques for CP-LTE and ZP-LTE Downlink Systems"* International Journal of Computer Networks & Communications (IJCNC) Vol.4, No.4, July 2012

[10] Asad Mehmood & Waqas Aslam Cheema *" CHANNEL ESTIMATION FOR LTE DOWNLINK"* MSc thesis, Blekinge Institute of Technology September, 2009

[11] 3GPP, TR 36.211 V8.7.0, *"Physical Channels and Modulation,"* Release 8, May 2009

[12] Lauro. *"Frame Structures in LTE-TDD and LTE-FDD,"* Internet:www.lteuniversity.com/ get_trained/ expert_opinion1/b/lauroortigoza/archive/2012/08/07/frame-structures-in-lte-tdd-and-lte-fdd.aspx, Aug 2012[Dec. 1, 2014]

[13] Houman Zarrinkoub. *Understanding LTE using MATLAB from Mathematical Modeling to Simulation and Prototyping*. United Kingdom: John Wiley & Sons, Ltd, 2014.

[14] Borko Furht, Syed A. Ahson. *Long Term Evolution: 3GPP LTE Radio and Cellular Technology*, CRC Press, Apr 23, 2009 - Technology & Engineering.

[15] Yong S. Cho, Jaekwon Kim, Won Y. Yang and Chung G. Kang. *MIMO-OFDM WIRELESS COMMUNICATIONS WITH MATLAB,* Singapore: John Wiley & Sons (Asia) Pte Ltd, 2010

[16] T. S. Rappaport, *Wireless Communications*, 2nd Edition, Prentice Hall, 2002

[17] S. B. Weinstein and P. M. Ebert, *"Data Transmission by Frequency-Division Multiplexing using the Discrete Fourier Transform," IEEE Trans. Commun. Techn.*, vol. COM-19, no. 5, pp. 628–634, Oct. 1971.

[18] K. Witrisal, *"OFDM Air-Interface Design for Multimedia Communications"*, Ch. 4, Ph.D. Thesis, Delft University of Technology, the Netherlands, April 2002

[19] A. Peled and A. Ruiz, *"Frequency Domain Data Transmission Using Reduced Computational Complexity Algorithms*," in Proc. IEEE Int. Conf. Acoust., Speech, Signal Processing , Denver, CO, 1980, pp. 964–967

[20] Rohde & Schwarz (July 2009)) *"Introduction to MIMO"* Application note [Online].

pp. 778-998. Available: www. http://cdn.rohde-schwarz.com/pws/dl_downloads/dl_application/application_notes/1ma142/1MA142_0e_introduction_to_MIMO.pdf [May. 1, 2015].

[21] G. Stüber, *Principles of Mobile Communication*, Kluwer, 2001.

[22] S. M. Alamouti, *"A simple transmit diversity technique for wireless communications,"* IEEE J. Select. Areas Commun., vol. 16, no. 8, pp. 1451–1458, Oct. 1998.

[23] Yao Chen, Emre Aktas, and Ufuk Tureli *"Optimal Space-Frequency Group Codes for MIMO-OFDM System"* Communications, IEEE Transactions on Vol.54, No. 3 ,pp. 553 – 562, March 2006

[24] P. Venkateswarlu. *"Channel Estimation techniques in MIMO OFDM LTE systems"* Int. Journal of Engineering Research and Applications ISSN: 2248-9622, Vol. 4, Issue 7(version1) July 2014, pp. 157-161

[25] Tufvesson, F. and Maseng, T. *"Pilot assisted channel estimation for OFDM in mobile cellular systems."* IEEE VTC'97, vol. 3, May 1997, pp. 1639–1643.

[26] Van de Beek, J.J., Edfors, O., Sandell, M. *" On channel estimation in OFDM systems."* IEEE VTC'95, vol. 2, July 1995, pp. 815–819.

[27]Coleri, S., Ergen, M., Puri, A. and Bahai, A. *"Channel estimation techniques based on pilot arrangement in OFDM systems."* IEEE Trans. on Broadcasting, 48(3), 223–229, 2002.

[28] Heiskala, J. and Terry, J. *OFDM Wireless LANs: A Theoretical and Practical Guide, SAMS.* 2002

[29] Hsieh, M. and Wei, C. "*Channel estimation for OFDM systems based on comb-type pilot arrangement in frequency selective fading channels."* IEEE Trans. Consumer Electron, 44(1), 217–228, 1998.

[30] Van Nee, R. and Prasad, R. *OFDM for Wireless Multimedia Communications*, Artech House Publishers, 2000.

[31] Lau, H.K. and Cheung, S.W. "*A pilot symbol-aided technique used for digital signals in multipath environments.*" IEEE ICC'94, vol. 2, May 1994, pp. 1126–1130.

[32] J. Vinogradova, N. Sarmadi, and M. Pesavento *"Subspace-based semi-blind channel estimation method for fast fading orthogonally coded MIMO-OFDM systems."* 2011 4th IEEE International Workshop on Computational Advances in Multi-Sensor Adaptive Processing.

[33] L. Tong, G. Xu, B. Hassibi, and T. Kailath, "*Blind identification and equalization of multipath channels: A frequency domain approach," IEEE* Trans. Inform. Theory, vol. 41, pp. 329–334, Jan. 1995.

[34] L. Tong, G. Xu, and T. Kailath, *"Blind identification and equalization based on second-order statistics: A time domain approach*," IEEE Trans.Inform. Theory, vol. 40, Mar. 1994.

[35] W.K. Ma, B.N. Vo, T. N. Davidson, and P.-C. Ching, "*Blind ML detection of orthogonal space–time block codes: Efficient high performance implementations,"* IEEE Trans. Signal Process., vol. 54, pp.738–751, Feb. 2006.

[36] J. Via and I. Santamaria, "*On the blind identifiability of orthogonal space–time block codes from second-order statistics*," IEEE Trans. Inf. Theory, vol. 54, pp. 709–722, Feb. 2008.

[37] F. Gao and A. Nallanathan, "*Blind channel estimation for MIMO OFDM systems via non redundant linear precoding,*" IEEE Trans.Signal Process., vol. 55, no. 2, pp. 784–789, Feb. 2007.

[38] C. Shin, R. W. Heath, and E. J. Powers, "*Blind channel estimation for MIMO-OFDM systems,*" IEEE Trans. Veh. Tech., vol. 56, pp. 70–685, Mar. 2007.

[39] T. Wo and P. A. Hoeher, "*Semi-blind channel estimation for frequency-selective MIMO systems,*" in Proc. 14-th IST Mobile & Wireless Commun. Summit, Dresden, Germany, June 2005.

[40] V. Buchoux, O. Cappe,´ E. Moulines, and A. Gorokhov, "*On the performance of semi-blind subspace-based channel estimation,*" IEEE Trans. Signal Proc.,vol. 48, pp. 1750–1759, June 2000.

[41] Kaveh Pahlavan. *Principles of Wireless Networks A unified approach*, Prentice hall PTR, 2002

[42] Dr. Abhijit Mitra , "*Mobile communication* ", Indian Institute of Technology, Guhati ECE,2007-2008

[43] 3GPP, TS 36.101 V11.2.0, "*UE Radio Transmissions and Reception*" Release 11, Sept 2012

[44] Moray Rumney. *LTE and the Evolution to 4G wireless design and Measurement challenges*, Second edition, United Kingdom: John Wiley & Sons, Ltd, 2013

[45] Mahmoud AMMAR, Bechir NSIRI, Walid HAKIMI and Messaoud ELJAMAI, *"A Comprehensive Study of Open-loop Spatial Multiplexing and Transmit Diversity for LTE Downling"* International Journal of Computer Networks & Communications (IJCNC) Vol.5, Issue.2, February 2014

[46] Berhard Schulz, Schwarz "*LTE Transmission Modes and Beamforming*" White Paper-1MA-186_0e, October 2011

[47] Abhijit Mitra. "Mobile Communication" Internet: www.iitg.ernet.in/scifac/qip/public_html/cd_cell/mobile_communication_index.htm [May,2014].